



Identification and development of thiazole leads as COX-2/5-LOX inhibitors through *in-vitro* and *in-vivo* biological evaluation for anti-inflammatory activity



Jaismy Jacob P, S.L. Manju

Department of Chemistry, School of Advanced Sciences, Vellore Institute of Technology, Vellore, Tamil Nadu, India

ARTICLE INFO

Keywords:

Anti-inflammatory activity
COX
LOX
Thiazole
Thiazolidene

ABSTRACT

Treatment of inflammation using NSAIDs is coupled with a risk of severe gastric adverse events. Development of dual COX-2/5-LOX inhibitors turns out to be an imperative area devoted to safer NSAIDs. A series of thiourea, thiazole, and thiazolidene derivatives were synthesized by green synthetic approach and COX-1, COX-2 and 5-LOX inhibition screening resulted in the identification of a potent compound **6I** with IC₅₀ of 5.55 μM, 0.09 μM, and 0.38 μM respectively. Compound **6I** made significant decrease (60.82%) in the carrageenan-induced edema in male Wistar rats. qRT-PCR analysis and determination of PGE₂ and LTB₄ in the rat paw tissues indicated that this thiazole based dual inhibitor significantly reduced the expression of COX-2 and 5-LOX genes besides the marked reduction in both PGE₂ and LTB₄ levels. The gastric safety profiling revealed an enhanced gastrointestinal safety of the compound **6I** on histopathological examination. Molecular docking studies at COX-2 and 5-LOX active sites were consistent with biological studies by significant protein-ligand interaction. Besides, results of *in-vitro* PGE₂ and LTB₄ studies on RAW 264.7 cells as well as antioxidant studies were parallel to the dual inhibitory activity. The present investigations identify a promising lead having anti-inflammatory potential with an improved gastric safety profile.

1. Introduction

In today's world, chronic inflammation and associated complications such as osteoarthritis and cancer have become the most challenging diseases which need special attention [1]. It is well known that alteration in the arachidonic acid pathway and overproduction of prostaglandins (PGs) and leukotrienes (LTs) are the root cause of chronic inflammation [2,3]. The up-regulation of COX-2 isoenzyme during inflammation and involvement of leukotrienes and lipoxins produced by lipoxygenases (LOX) in bronchial asthma pathogenesis and edema development clearly explains the role of these enzymes in inflammation [4]. Non selective inhibition of constitutive form of cyclooxygenase, viz COX-1 alone or combined COX-1 and COX-2 inhibition is responsible for the severe adverse effects of NSAIDs [4]. Gastric side effects associated with traditional NSAIDs and withdrawal of selective COX-2 inhibitors such as valdecoxib and rofecoxib from medical use due to cardiovascular events makes the inflammation treatment

more complex [5,6]. So far, the only approved 5-LOX inhibitor for clinical use is zileuton. But its use is limited because of poor pharmacokinetics and hepatotoxicity [7]. In the investigation for new drugs devoid of side effects while retaining high anti-inflammation potency, the unique dual COX-2/5-LOX inhibitory concept has been introduced. Accordingly, several dual inhibitors have been reported but they are in different phases of clinical trials. Licofelone, **1** is an interesting dual COX/LOX inhibitor in phase III clinical trial for osteoarthritis that inhibit COXs non-selectively with COX IC₅₀ = 0.21 μM and 5-LOX activating protein (FLAP) with 5-LOX IC₅₀ = 0.18 μM [8]. Two other molecules with significant dual activity identified are tepoxalin, **2** approved for veterinary use [9] and darbufelone, **3** which is in phase III clinical trial for rheumatoid arthritis [10]. Tenidap, **4** is a cytokine modulating anti-rheumatic drug with COX/5-LOX inhibition that was more active than conventional NSAIDs in the clinical treatment of rheumatoid arthritis, but its development was halted due to kidney and liver toxicity [11]. Structures of dual COX and LOX inhibitors were

Abbreviations: COX-1, cyclooxygenase-1; COX-2, cyclooxygenase-2; 5-LOX, 5-lipoxygenase; NSAID, non steroidal anti-inflammatory agent; PGE₂, prostaglandin E₂; LTB₄, leukotriene B₄; qRT-PCR, quantitative real-time polymerase chain reaction; GAPDH, Glyceraldehyde-3-phosphate dehydrogenase; LPS, Lipopolysaccharide; ip, intraperitoneal; FLAP, 5-lipoxygenase activating protein; ROS, reactive oxygen species; DPPH, 2,2-diphenyl-1-picrylhydrazyl; NO, nitric oxide; PBS, phosphate-buffered saline

E-mail addresses: jaismyjacobp@gmail.com (J. Jacob P), slmanju@vit.ac.in (S.L. Manju).

<https://doi.org/10.1016/j.bioorg.2020.103882>

Received 3 January 2020; Received in revised form 13 April 2020; Accepted 22 April 2020

Available online 25 April 2020

0045-2068/ © 2020 Elsevier Inc. All rights reserved.

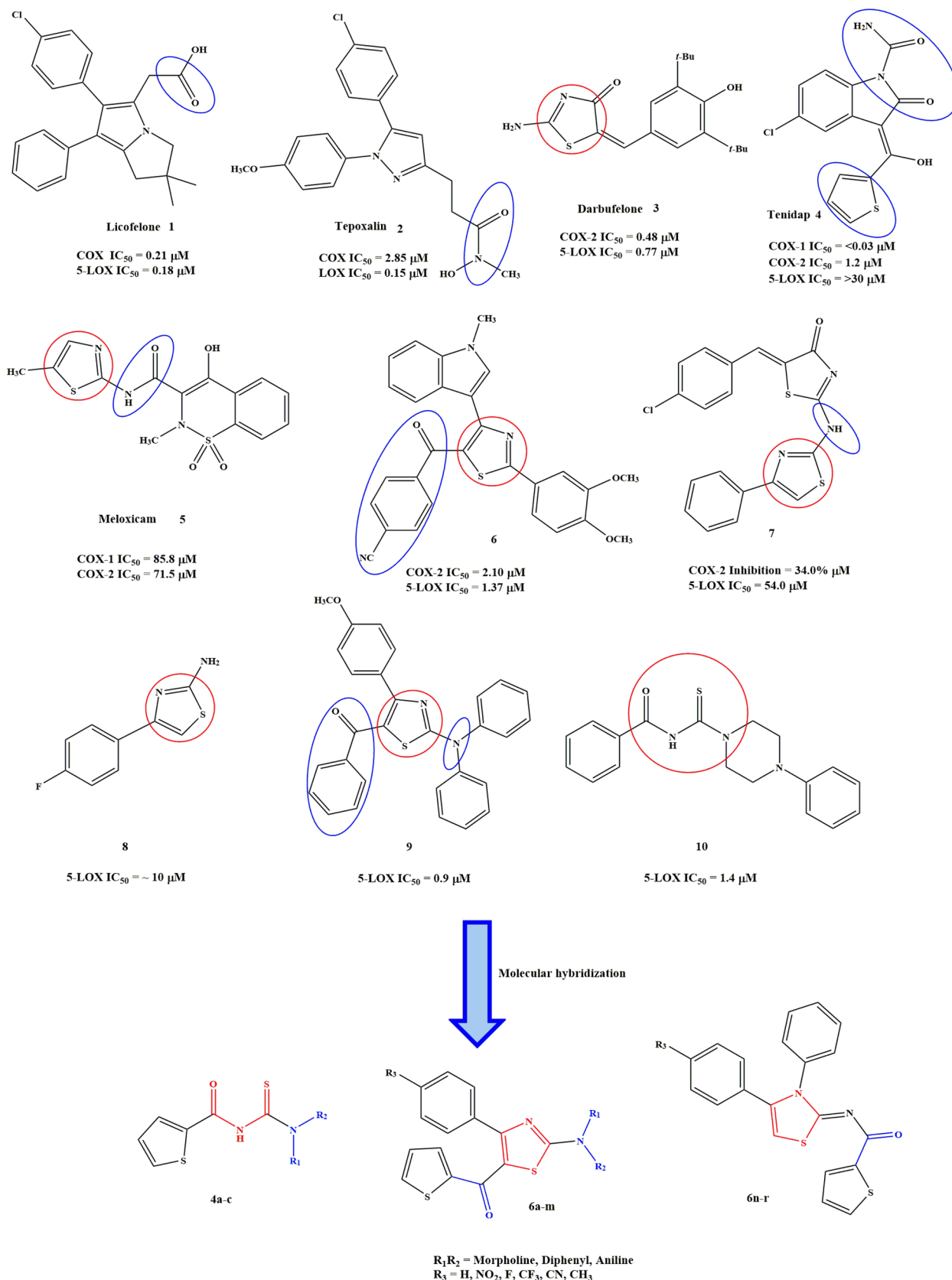
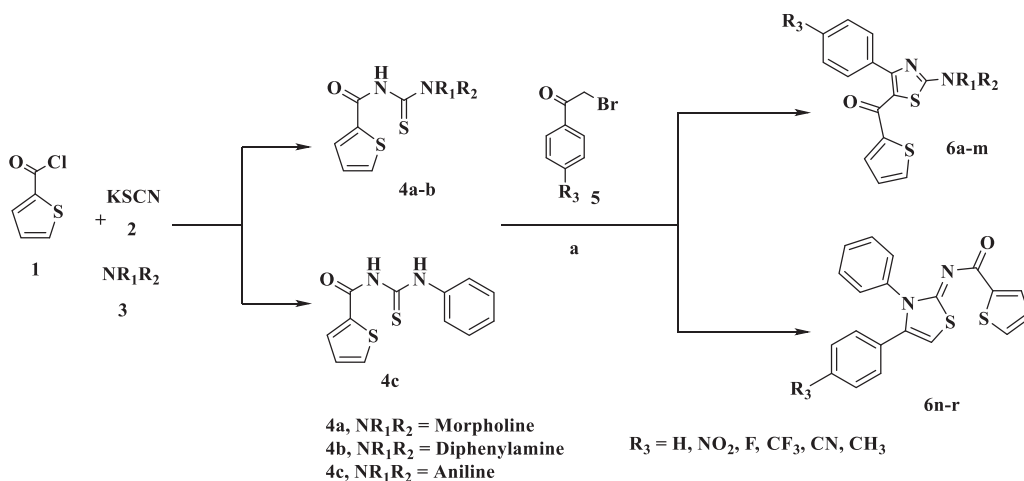


Fig. 1. Structures of some dual COX/LOX inhibitors in clinical trials, dual COX-2/5-LOX inhibitors, 5-LOX inhibitors and newly designed molecules. Potential functional groups for dual COX-2/5-LOX activity and thiazole ring are shown in circles.



Scheme 1. Synthesis of N-(amino-4-carbamothioyl)thiophene-2-carboxamide **4a-c**, (2-amino-4-phenylthiazol-5-yl)(thiophen-2-yl)methanone **6a-m** and N-(3-phenyl-4-(4-(substituted)phenyl)thiazol-2(3H)-ylidene)thiophene-2-carboxamide **6n-r**, reagents and reaction conditions: (1) 2-thiophenecarbonyl chloride, (2) potassium thiocyanate, (3) morpholine, diphenylamine, aniline, (a) water, 0.1 equiv TBAF, room temperature, 1 h, then heat at 80 °C, 2 h.

shown in Fig. 1. Recently, indole-2-amide derivatives were reported by Li et al. as dual COX-2/5-LOX inhibitors with marked *in-vitro* and *in-vivo* anti-inflammatory potential [12]. Hybrids of diaryl-1,5-diazoles and morpholines with CF₃ and SO₂NH₂ substituted phenyl rings showed significant *in-vitro* dual inhibition and anti proliferative activity [13]. In spite of the intense research in this regard, so far no dual COX-2 and 5-LOX inhibitor could be accomplished clinically. Hence, the designing of novel pharmacophores with dual COX-2 and 5-LOX inhibition would pave a new therapeutic option for anti-inflammatory therapy with an enhanced safety profile.

Thiazole is a unique five-membered heterocyclic compound with a variety of therapeutic utility such as anti-inflammatory, antioxidant [14,15], anticancer [16] and anti-HIV [17] properties etc. Moreover, a variety of drugs such as suphathiazole, niridazole, thiabendazole, faretinole and preferential COX-2 inhibitor meloxicam, **5** (Fig. 1) possess thiazole ring in their structure. Recently, 1,2-benzisothiazol-3(2H)-one-1,1-dioxides were screened for their COX-1/COX-2 inhibition and found to possess similar activity to celecoxib. *In-vivo* anti-inflammatory and antiulcer property of the above compounds were significant with ~ 60% inhibition of edema [18]. Sathya et al. designed and synthesized 2, 4-bis(aryl/heteroaryl)-5-acylthiazole, **6** (Fig. 1) as dual inhibitors of COX-2 and 5-LOX with COX-2 IC₅₀ = 2.10 μM and 5-LOX IC₅₀ = 1.37 μM respectively. Furthermore, a combination of thiazolidinone and thiazole rings, compound **7** (Fig. 1) showed 67.3% protection on *in-vivo* anti-inflammatory models [19]. Recently, our group reported substituted 2-amino thiazole derivatives as potent 5-LOX inhibitors and effective anti-inflammatory agents. The compounds **8**, **9**, and **10** (Fig. 1) have shown considerable inhibition of 5-LOX (IC₅₀ ~ 10 μM, 0.9 μM and 1.4 μM respectively) and appreciable anti-inflammatory activities [20,21]. These thiazole analogues showed equivalent potency with that of zileuton (IC₅₀ ~ 1.5 μM), a selective 5-LOX inhibitor [22]. In the present work, newly designed molecules combined the pharmacophore requirements of dual COX-2 and 5-LOX inhibitor.

As a continuation and modification of our earlier work [20], herein we report the design and novel green synthesis of 2-(substituted)-4-(4-substituted phenyl)thiazol-5-yl)(thiophen-2-yl)methanone **6a-m** and N-(3-phenyl-4-(4-(substituted phenyl)thiazol-2(3H)-ylidene)thiophene-2-carboxamide **6n-r** as dual COX-2/5-LOX inhibitors (Fig. 1) Considering peculiarly larger COX-2 active site, a 4-phenyl group along with a 5-thiophene-2-carbonyl group was introduced into the thiazole and thiazolidene nucleus which can selectively bind to the secondary pocket and give sufficient steric bulk to block the COX-2 hydrophobic channel. At 5-LOX enzyme, 2-substituted secondary amine and 5-thiophenyl-2-carbonyl group in the thiazole ring provides H-bond acceptor and hydrophobic centroid features respectively to the molecule. N-hydroxy urea group of the zileuton is incorporated in the scaffold in its isosteric

form viz thiourea and designed a series of compounds, **4a-c** (Fig. 1). Further, structural modifications such as N-substitution of secondary amine and electron releasing and withdrawing substitutions at *p*-phenyl are done to optimize the anti-inflammatory efficacy of the molecules, **6a-r**.

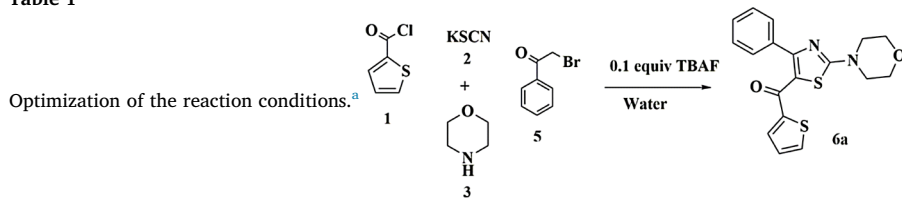
This work provided a one-pot multi-component green synthetic method for thiazole and thiazolidene derivatives. The *in-vitro* inhibitory activities of target compounds for COX-1, COX-2, 5-LOX, PGE₂ and LTB₄ have been evaluated. Further, *in-vivo* anti-inflammatory and anti-ulcer potential were studied. In order to explore the mechanism of selective COX-2 and 5-LOX inhibition, gene expression studies by quantitative real-time polymerase chain reaction (qRT-PCR) were performed successfully on rat paw tissues. Besides, active site binding interactions of the most active molecule on COX-2 and 5-LOX enzymes were explored by molecular modeling.

2. Results and discussion

2.1. Chemistry

The multi-component one-pot green synthesis of N-(substituted carbamothioyl)thiophene-2-carboxamide **4a-c** [23–29], (2-(substituted)-4-(4-substituted phenyl)thiazol-5-yl)(thiophen-2-yl)methanone **6a-m** and N-(3-phenyl-4-(4-(substituted phenyl)thiazol-2(3H)-ylidene)thiophene-2-carboxamide **6n-r** is accomplished as depicted in Scheme 1 by a modified green synthetic route. The present synthesis is a modification of our previous work where cetyltrimethylammonium bromide (CTAB), a phase transfer catalyst was used for the synthesis of thiourea from acyl chloride, potassium thiocyanate and amines using toluene: water system. This study attempted to carry out a simple and efficient method of one pot green synthesis using tetrabutylammonium fluoride (TBAF) for N and S heterocyclics in water. Reaction conditions were optimized by conducting a model reaction using thiophene-2-carbonyl chloride, potassium thiocyanate, morpholine and phenacyl bromide. Comparison reactions were performed using similar catalysts such as tetrabutylammonium bromide (TBAB), tetrabutylammonium hydrogensulphate (TBAHS) and CTAB (Table 1). Optimal reaction conditions showed that water acted as a suitable solvent not only in terms of yield but also in its environmental safety, easy to handle and cost-effectiveness. The entire reaction was carried out in a single pot containing water and TBAF. Briefly, 2-thiophenecarbonyl chloride and potassium thiocyanate were added to aq. solution of 0.1 equiv of TBAF to afford thiophene-2-carbonylisothiocyanate. These isothiocyanates were further converted to corresponding N-(substituted carbamothioyl)thiophene-2-carboxamide by adding secondary amine and stirring for 1 h at RT. Addition of equivalent amounts of phenacyl bromides to the reaction mixture containing thiourea and reflux at 80 °C for 2 h resulted

Table 1

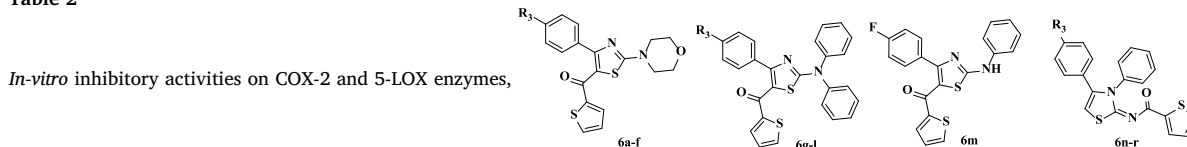


Sl no	Solvent	Catalyst	Temperature (°C)	Time (h)	Yield %
1	Water	–	RT	24	–
2	Water	–	60	24	–
3	Water	–	Reflux	24	10
4	Water	TBAF	RT	5	45
5	Water	TBAF	60	3	72
6	Water	TBAF	80	2	91
7	Water	TBAB	80	3	88
8	Water	TBAHS	80	3.5	80
9	Water	CTAB	80	3.5	80
10	DMSO	TBAF(0.1)	80	2	25
11	DMF	TBAF(0.1)	80	2	0
12	Ethanol	TBAF(0.1)	80	2	80
13	Acetonitrile	TBAF(0.1)	80	2	76

^a Isolated yields.

in lead molecules **6a-m**. This method followed a novel route of [3 + 2] Hantzsch thiazole synthesis. Interestingly, according to the literature, the addition of phenacyl bromides to the monosubstituted thiourea, **4c** resulted in thiazolidene derivatives, **6n-r** rather than thiazole at the same reaction conditions (Scheme 1) [30]. But reaction between **4c** and 4-fluorophenacyl bromide followed [3 + 2] thiazole synthesis and formed **6m**, a thiazole. The thioureas (**4a-c**) formed as an intermediate were separated and purified for the purpose of biological screening. This green synthetic methodology was further extended to various *N*-disubstituted and monosubstituted thioureas and phenacyl bromides substituted with electron-withdrawing and electron-donating groups.

Table 2



Compound	<i>R</i> ₃	IC ₅₀ ± SD (μM)	
		COX-2	5-LOX
4a [23,24]	–	–	8.39 ± 1.51
4b [25–27]	–	83.24 ± 3.32	7.66 ± 0.26
4c [28,29]	–	6.23 ± 0.66	8.35 ± 0.16
6a [23]	H	60.59 ± 2.9	6.02 ± 0.17
6b	NO ₂	0.55 ± 0.02	5.07 ± 0.1
6c	F	3.77 ± 0.13	6.46 ± 0.28
6d	CF ₃	3.62 ± 0.51	6.58 ± 0.05
6e	CN	4.75 ± 0.45	6.61 ± 0.19
6f	CH ₃	5.88 ± 0.03	6.65 ± 0.385
6g	H	3.92 ± 0.25	7.60 ± 0.75
6h	NO ₂	0.61 ± 0.01	4.20 ± 0.12
6i	F	4.03 ± 0.18	0.58 ± 0.03
6j	CF ₃	0.62 ± 0.01	0.39 ± 0.01
6k	CN	6.48 ± 0.11	0.57 ± 0.04
6l	CH ₃	0.09 ± 0.002	0.38 ± 0.01
6m	F	6.23 ± 0.36	8.11 ± 0.15
6n	H	54.09 ± 0.41	6.15 ± 0.80
6o	NO ₂	0.77 ± 0.12	0.58 ± 0.04
6p	CF ₃	0.45 ± 0.04	9.39 ± 1.02
6q	CN	6.64 ± 0.12	5.73 ± 0.25
6r	CH ₃	0.89 ± 0.01	4.96 ± 0.75
Etoricoxib	–	0.07 ± 0.007	–
Zileuton	–	–	0.14 ± 0.01

^aIC₅₀ value is the compound concentration required to inhibit 50% of COX-2 or 5-LOX.

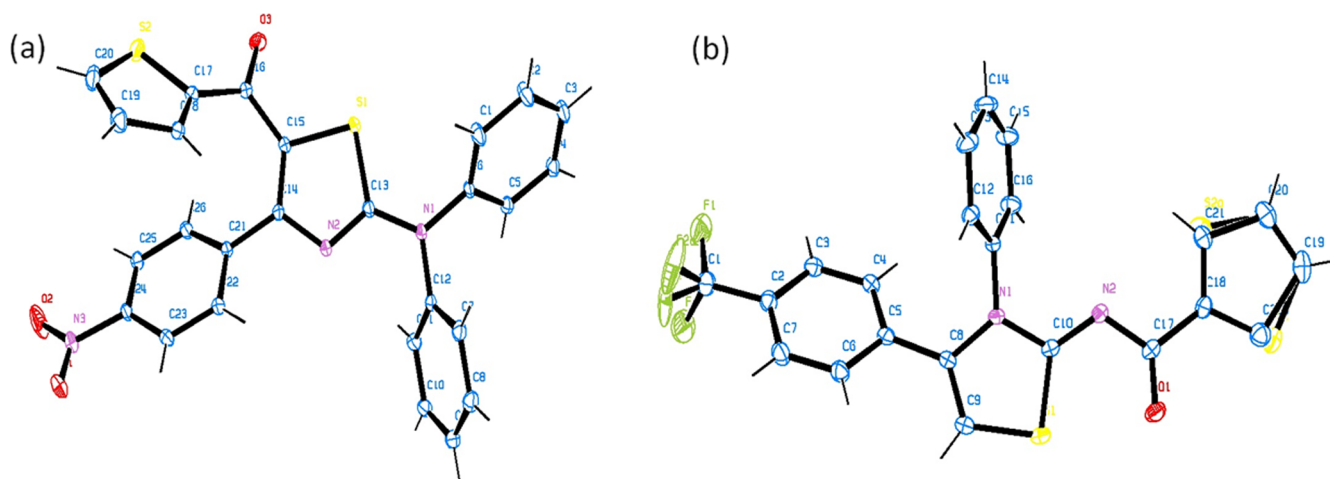


Fig. 2. (a) ORTEP diagram of compound **6h**, CCDC no. 1951604. (b) ORTEP diagram of compound **6p**, CCDC no. 1959072. In this structure because of high torsion, flipping occurs between S₂ and C₂₁ part of the molecule. Disordered F₂ was observed due to rotation.

Table 3

In-vitro inhibitory activities of selected compounds on COX-1 and COX-2, IC₅₀ values and selectivity Indices (SI).

Compound	IC ₅₀ ± SD (μM) ^a		Selectivity Index (SI)
	COX-1	COX-2	
6b	8.14 ± 0.81	0.55 ± 0.02	14.5
6h	8.05 ± 1.32	0.61 ± 0.01	13.19
6j	6.30 ± 0.40	0.62 ± 0.01	10.16
6l	5.55 ± 0.77	0.09 ± 0.002	61.66
6o	6.42 ± 0.71	0.77 ± 0.12	8.34
6r	6.05 ± 1.30	0.89 ± 0.01	6.79
Etoricoxib	6.39 ± 0.83	0.07 ± 0.007	91.28

^bSI: IC₅₀ (COX-1)/IC₅₀ (COX-2).

^a IC₅₀ value is the compound concentration required to inhibit 50% of COX-1 or COX-2.

protons. Compounds **6a-f** showed two triplets of morpholine hydrogen at ~ 3.63 and 3.84 ppm respectively with integration of four each. Aromatic protons were present in the range of 6.765–8.106 ppm confirming the formation of expected thiazoles/thiazolidenes. The ¹³C NMR displayed two prominent peaks at ~ 180 and 170 ppm ascribed to carbonyl carbon and C-2 of thiazole ring respectively, whereas in ¹³C NMR of thiazolidene series, carbonyl carbon and C-2 of thiazolidene peak were observed at 169 and 168 ppm respectively. In general, when phenacyl bromides substituted with electron withdrawing groups exhibited fast reaction rate and good yield. The ORTEP diagrams of compound **6h** and **6p** with CCDC no. 1951604 and 1959072 are presented in Fig. 2. The thiazole moiety formed by this reaction was undergoing a rearrangement and instead of an expected phenyl methanone substitution at C-5 of thiazole ring, surprisingly, we found thiophenyl methanone substitution at C-5. Interestingly, this method offers a specific technique which could be applied to introduce a variety of substitution at C-5 of thiazole ring using different aryl or heteroaryl acid chlorides. Alternatively, monosubstituted acylthiourea viz N-(phenylcarbamothioyl)thiophene-2-carboxamide (**4c**) produced thiazolidenes consistent with previous reports [24,30].

2.2. COX-1, COX-2 and 5-LOX enzyme inhibitory activity

COX-2 and 5-LOX inhibitory screening assays were conducted on all the compounds, **4a-c** and **6a-r**. The COX inhibitory activity was eventually measured by determining the amount of PG synthesized by the enzyme in the presence of test compounds at different concentrations. Herein, the concentration of the inhibitor present and the amount of PG

Table 4

In-vitro PGE₂ and LTB₄ inhibitory activities in LPS-challenged RAW 264.7 cells.^a

Compound	IC ₅₀ ± SD (μM)	
	PGE ₂	LTB ₄
6b	7.87 ± 0.59	0.89 ± 0.02
6h	0.36 ± 0.09	0.72 ± 0.04
6j	0.94 ± 0.03	0.36 ± 0.02
6l	0.48 ± 0.07	0.28 ± 0.02
6o	6.32 ± 0.91	0.96 ± 0.06
6r	4.76 ± 0.47	0.58 ± 0.02
Etoricoxib	0.44 ± 0.07	–
Zileuton	–	0.47 ± 0.02

^aIC₅₀ value is the compound concentration required to produce 50% inhibition of PGE₂ and LTB₄.

released in each well are inversely proportional. Among them, best six compounds with significant percentage inhibition for COX-2 and 5-LOX were selected for further COX-1 IC₅₀ determination. Compound **6l** showed excellent selectivity towards COX-2 with IC₅₀ = 0.09 ± 0.002 μM, whereas IC₅₀ for COX-1 was 5.55 ± 0.77 μM. The selectivity index of the most potent compound **6l** (SI = 61.66) was superior to remaining compounds and comparable to that of etoricoxib (COX-2 IC₅₀ = 0.07 ± 0.007 μM, SI = 91.28), a selective COX-2 inhibitor (Table 3). Among the synthesized precursor and target compounds, thiourea derivatives exhibited poor COX-2 inhibition. Similarly, thiazoles with no substitution on *p*-phenyl ring at C-4 of thiazole ring (R₃) showed less activity. Among thiazole derivatives, diphenylamino thiazoles have shown better COX-2 inhibition than morpholine derivatives. In comparison to thiazole compounds thiazolidene derivatives also exhibited significant COX-2 inhibition especially when R₃ was substituted with electron withdrawing groups (NO₂ and CF₃). The exceptional selectivity and activity of (2-(diphenylamino)-4-(*p*-tolyl)thiazol-5-yl)(thiophen-2-yl)methanone, **6l** to COX-2 over COX-1 could be due to more surrounding aromatic rings on thiazole ring which afforded bulkiness to the molecule. Though the substituents of the most active compounds are diverse, the tertiary amino group and *p*-phenyl substitution on central thiazole ring play a major role in the anti-inflammatory activity. Generally, compounds with both electron-withdrawing and donating groups at R₃ showed significant COX-2 inhibition.

5-LOX inhibitory screening was carried out for all the compounds synthesized. *In-vitro* 5-LOX screening assay measures the amount of hydroperoxides produced during the lipoxygenation reaction by purified 5-lipoxygenase enzyme. It is a sensitive method to detect

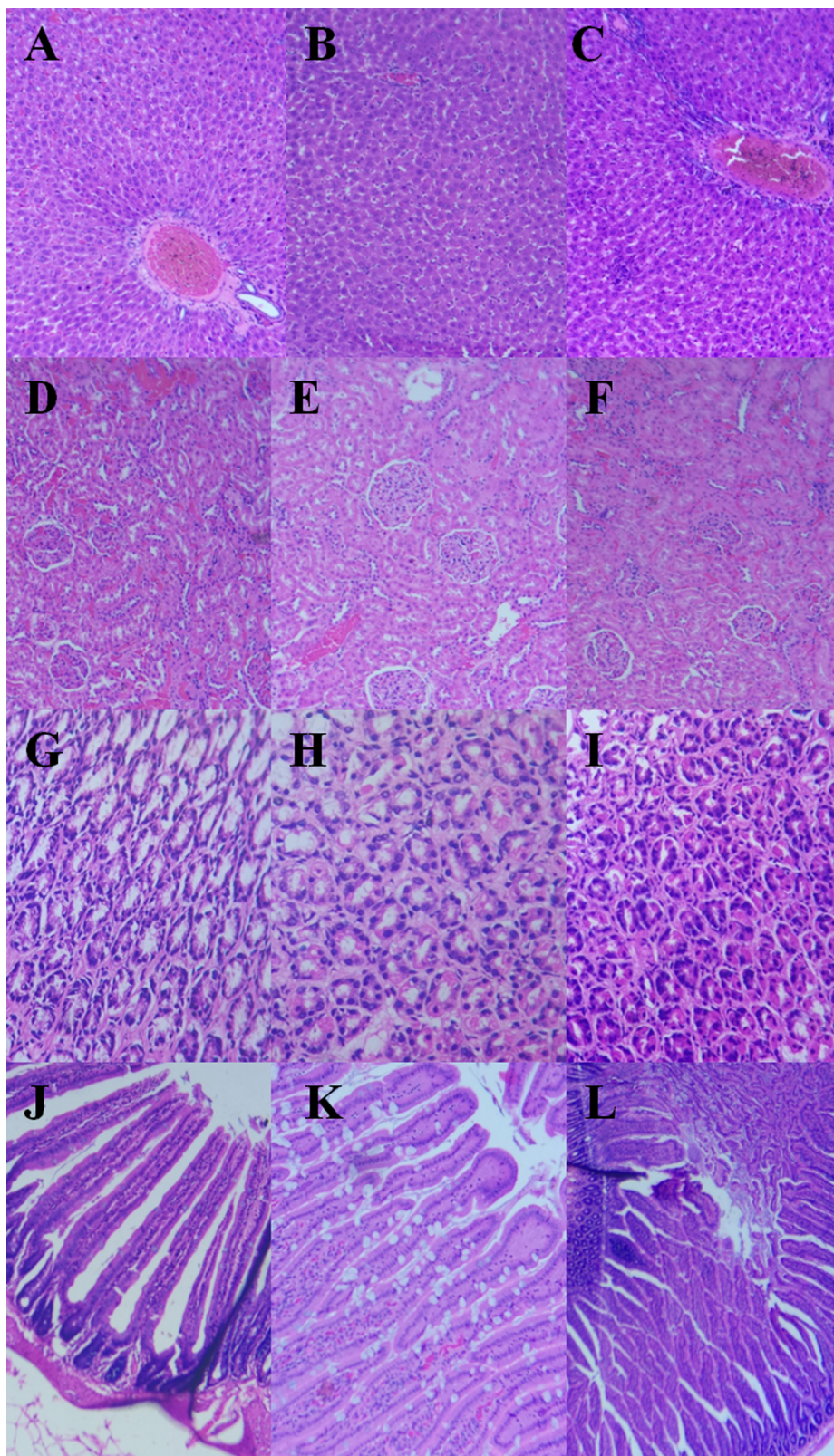


Fig. 3. A, D, G, J- Histology of liver, kidney, stomach, and intestine of control (400 \times). B, E, H, K- Histology of liver, kidney, stomach, and intestine at a dose of 500 mg/kg after compound **6l** treatment (400 \times). C, F, I, L- Histology of liver, kidney, stomach, and intestine at a dose of 2000 mg/kg after compound **6l** treatment (400 \times).

hydroperoxide at different positions within the fatty acid of any carbon length. Results demonstrated appreciable 5-LOX inhibition for compound **6l** ($IC_{50} = 0.38 \pm 0.01 \mu M$) and **6j** ($IC_{50} = 0.39 \pm 0.01 \mu M$).

The standard drug zileuton showed $IC_{50} = 0.14 \pm 0.01 \mu M$. Thiazolidene derivative **6o**, with NO_2 group at R_3 showed significant 5-LOX inhibition with $IC_{50} = 0.58 \pm 0.04 \mu M$. The thiazole derivatives

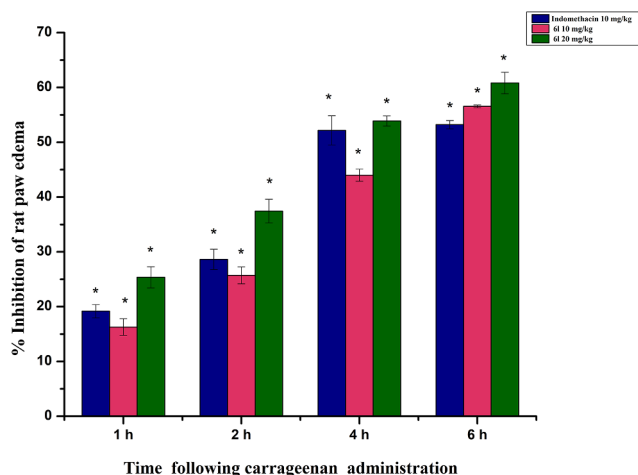


Fig. 4. Effect of compound **61** on carrageenan-induced inflammation model in rat paw tissue. All values are expressed as the mean \pm SEM (n = 5). One way ANOVA was used to calculate statistical significance. *p < 0.050 vs control group.

with diphenylamine substitution at C-2 of thiazole ring have better biological profile compared to other compounds in the series. The results are displayed in Table 2.

2.3. PGE₂ and LTB₄ inhibitory activity in LPS challenged RAW 264.7 cell lines

The levels of PGE₂ and LTB₄ were considerably up-regulated in LPS-challenged macrophage RAW 264.7 cells. After LPS induction, PGE₂ and LTB₄ levels in the wells were increased from 0.04 to 1.28 pg/ml and 0.03 to 0.92 pg/ml respectively. All the tested compounds inhibited both PGE₂ and LTB₄ in a concentration-dependent manner. Compound **61** inhibited PGE₂ synthesis with IC₅₀ = 0.48 \pm 0.07 μ M and LTB₄ synthesis at IC₅₀ = 0.28 \pm 0.02 μ M, whereas, selective COX-2 inhibitor, etoricoxib exhibited PGE₂ inhibition at IC₅₀ = 0.44 \pm 0.07 μ M and 5-LOX inhibitor, zileuton showed LTB₄ inhibition at IC₅₀ = 0.47 \pm 0.02 μ M (see Table 4). These inhibitory studies displayed the inhibitory potency of synthesized compounds towards PGE₂ and LTB₄ beyond any doubt.

Compound **61** has shown promising anti-inflammatory potential among the synthesized compounds with significant inhibition of COX-2, 5-LOX, PGE₂ and LTB₄. Hence compound **61** was chosen for further biological studies.

2.4. In-vivo studies

2.4.1. Acute toxicity studies

In-vivo acute toxicity study of compound **61** was performed on male Wistar rats as per OECD guidelines to scrutinize the toxic effects. The animals were administered with compound **61** at oral doses of 50, 500 and 2000 mg/kg. The animals were observed carefully and continuously for the first four hours for any signs of toxicity and thereafter at regular intervals on the first day. Afterwards, the animals were examined daily once for fourteen days. The animals were forfeited after 14 days and histological examination of kidney, liver, stomach, and intestine did not show any significant structural variation in comparison to control (Fig. 3).

2.4.2. In-vivo anti-inflammatory activity and gastric safety profiling

Gastric ulceration and bleeding are the most important side effects of NSAIDs. So compound **61** exhibiting promising *in-vitro* COX-2/5-LOX inhibition was further studied for *in-vivo* anti-inflammatory activity and its ulcerogenic potential. A rational study was designed on male Wistar

rats, in which rats were subjected to antiulcer study and anti-inflammatory study subsequently.

Carrageenan induced rat paw edema bioassay is a standard method for studying anti-inflammatory properties of the test molecule. After 1 h of oral administration of test and standard compounds, acute inflammation was induced on hind paws by intraplantar injection of 1% w/v carrageenan. The paw thickness was measured and anti-inflammatory activity was displayed as percentage inhibition of inflammation at time intervals 1, 2, 4 and 6 h, results are displayed in Fig. 4. Anti-inflammatory study of compound **61** revealed significant inhibition of edema (60.82 \pm 1.96%) in comparison to control and indomethacin (53.21 \pm 0.76%) after 6 h. The test compound showed a gradual and remarkable dose-dependent increase in anti-inflammatory activity during the study period. But, when the dose of **61** increased from 10 to 20 mg/kg there was a trivial improvement in the observed inhibitory activity pointing to the saturation of receptors at given doses.

Gross observation of the gastrointestinal mucosa following oral administration of compound **61** at 10 and 20 mg/kg illustrated a normal stomach texture whereas indomethacin 10 mg/kg treatment produced redness and ulceration in the gastric mucosa. In addition, histopathological examination of the treated rat stomachs was carried out to assess the degree of inflammatory response produced in the gastric layers. The results are displayed in Fig. 5. The histopathological examination demonstrated a normal histology for the compound **61** which ensured its gastrointestinal safety and potential medicinal value, whereas rats treated with indomethacin developed severe mucosal sloughing, granulation tissue and lymphocytic infiltrate showing its potential for ulceration.

2.5. PGE₂ and LTB₄ inhibitory activity in rat paw tissues during carrageenan-induced edema

Besides inhibition of rat paw swelling, the anti-inflammatory activity of compound **61** was confirmed by a variety of biochemical assays. The carrageenan-induced rat paw edema was coupled with a marked increase in PGE₂ and LTB₄ levels. After intraplantar injection of carrageenan, the PGE₂ levels in the hind paws of control animals showed a 10 fold increase over 0 to 6 h. The LTB₄ levels also increased markedly but lesser (6 fold) compared to PGE₂ at the same time interval. Pre-treatment with compound **61** showed a remarkable reduction in both PGE₂ and LTB₄ levels in the hind paw. Compound **61** at 10 mg/kg proved to be a more potent inhibitor of PGE₂ and LTB₄ synthesis than indomethacin 10 mg/kg. Results are depicted in Fig. 6.

2.6. qRT-PCR studies

Gene expression studies were performed on rat paw tissues following to anti-inflammatory screening to explore the gene expression level mechanism of the anti-inflammatory activity of compound **61**. Gene expressions of all the target genes were normalized with an endogenous control (GAPDH); subsequently, the expression of COX/LOX genes in the treated groups was normalized with that in the control group. COX-1, COX-2, and 5-LOX genes up-regulated their expression significantly (p < 0.050) at 6.6, 4.8, and 9.0 fold respectively as shown in Fig. 7. However, the expression of all the studied genes was significantly reduced in treated rats. Interestingly, a concentration-dependent activity was observed with compound **61** as 20 mg/kg was more efficient in controlling the gene expression compared to lower dose treatment, 10 mg/kg. In addition, compound **61** significantly reduced the expression of genes in comparison to indomethacin 10 mg/kg especially against COX-2, where it was down-regulated (p < 0.050). COX-1 gene expression was not affected greatly with compound **61** treatment whereas 2.7 fold increases was observed with indomethacin. Thus, these molecules could be used as promising leads for anti-inflammatory therapy.

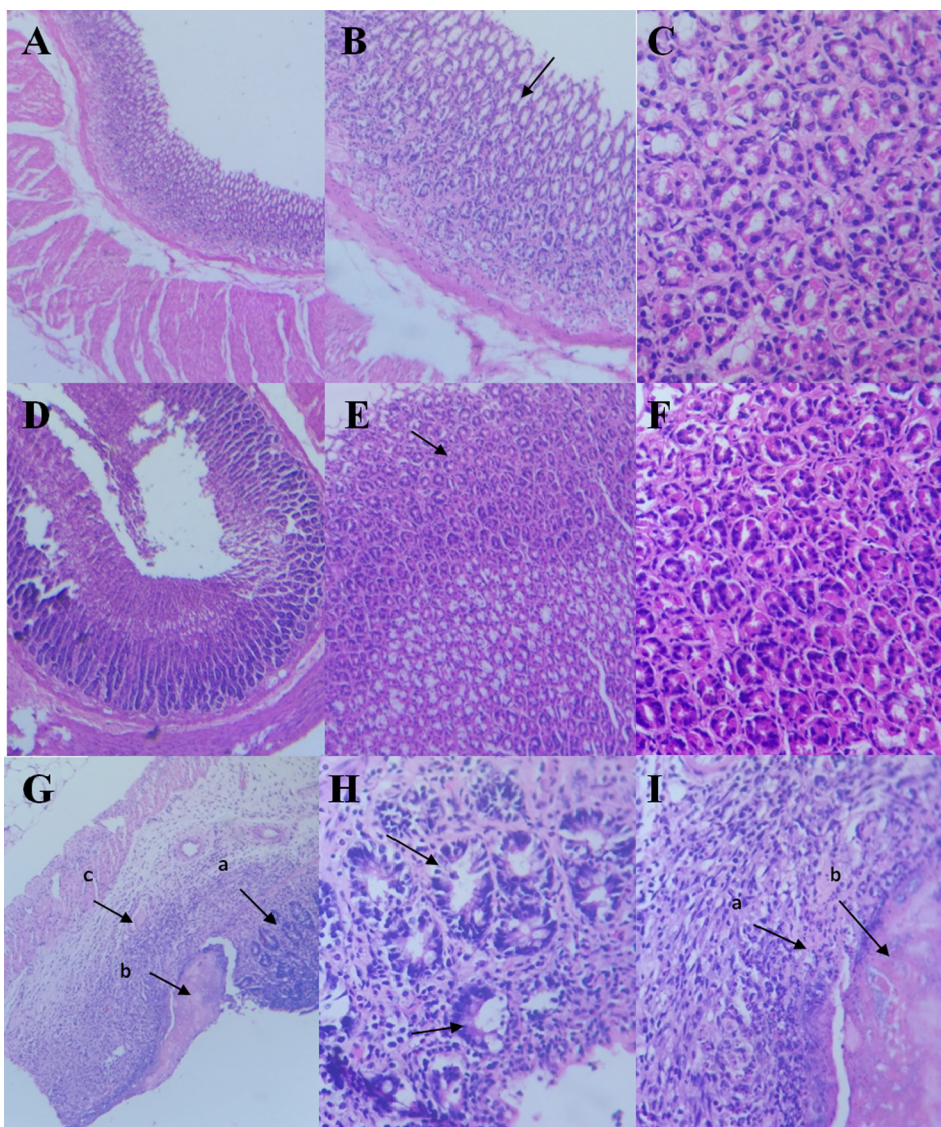


Fig. 5. 1. Histology of gastric mucosa of control rats (A) showing normal stomach mucosa (100x), (B) normal stomach architecture showing the surface mucous cells extending into gastric pits (arrow) (200×), (C) normal adjacent gastric mucosa, (400×). 2. Histology of gastric mucosa of rats treated with **6l** at 20 mg/kg (D) showing normal stomach mucosa (100×), (E) normal stomach architecture showing the surface mucous cells extending into gastric pits (arrow) (200×), (F) normal adjacent gastric mucosa, no evidence of gastric ulceration, (400×). 3. Histology of gastric mucosa of rats treated with indomethacin 10 mg/kg (G) Gastric mucosa with ulceration (a), sloughing of mucosal surface (b), granulation tissue and mucosal acute on chronic inflammatory infiltrate (c) (arrows), (100×), (H) mucosal lymphocytic infiltrates in the background of developing chronic gastritis, (arrows) (400×), (I) acute on chronic inflammatory granulation tissue with ulceration, (400×).

2.7. Antioxidant activity

Reactive oxygen species (ROS) is one of the root causes of inflammation and cancer. Antioxidants play a crucial role in interfering the production as well as inactivation of ROS. Mostly free radical scavengers and antioxidants facilitate anti-inflammatory therapy. [31] Results of the antioxidant study are duly presented in Fig. 8.

2.7.1. DPPH radical scavenging assay

Radical scavenging activity and anti-inflammatory efficacy have been proved to have a burly correlation. 2,2-Diphenyl-1-picrylhydrazyl (DPPH) radical scavenging activity of all the compounds at a concentration of 20 μM was evaluated. Majority of the compounds showed less antioxidant activity in comparison to standard, ascorbic acid (85.04 \pm 1.06%) except for compound **4a** and **6m**, which manifested significant free radical scavenging as that of standard, with 86.47 \pm 1.55% and 83.55 \pm 1.38% scavenging respectively. Whereas, most active dual-acting inhibitor, **6l** exhibited relatively lower DPPH scavenging activity (48.85 \pm 0.27%) similar to indomethacin (55.49 \pm 0.93%) and etoricoxib (57.19 \pm 0.27%) indicating that these molecules possibly proceeds through a non-redox mechanism. In this study, strangely enough, we couldn't find any linearity between anti-inflammatory potency and antioxidant activity because of exceptionally variant free radical scavenging activity

[32,33].

2.7.2. H_2O_2 radical scavenging assay

Compound **6h** showed the maximum percentage of H_2O_2 radical scavenging (70.33 \pm 1.97%) followed by **6l** which showed 62.94 \pm 1.75% scavenging activity at 20 μM concentration. Etoricoxib and indomethacin had 51.93 \pm 1.25% and 49.45 \pm 0.22% of H_2O_2 scavenging activity respectively. Ascorbic acid showed 21.86 \pm 0.68% H_2O_2 scavenging activity. In this study, molecules act either as electron or proton donors to reduce H_2O_2 to H_2O [34].

2.7.3. Iron chelating assay

The iron chelating activity of all the synthesized compounds was screened at 20 μM concentration. Among the compounds, *N*-(substituted carbamothioyl)thiophene-2-carboxamide derivatives (**4a-c**) showed high iron-binding capability (~62%) compared to thiazole and thiazolidene derivatives. Compound **6l** exhibited moderate iron chelating activity (44.50 \pm 1.06%). Even though the majority of the 5-LOX inhibitors act by inhibiting oxidation of ferrous (Fe^{2+}) to ferric (Fe^{3+}) we couldn't establish linearity between 5-LOX activity and iron chelating activity for compounds with 5-LOX inhibition. The iron binding activity of **4a-c** could be because of the thiourea group present in the molecule [35].

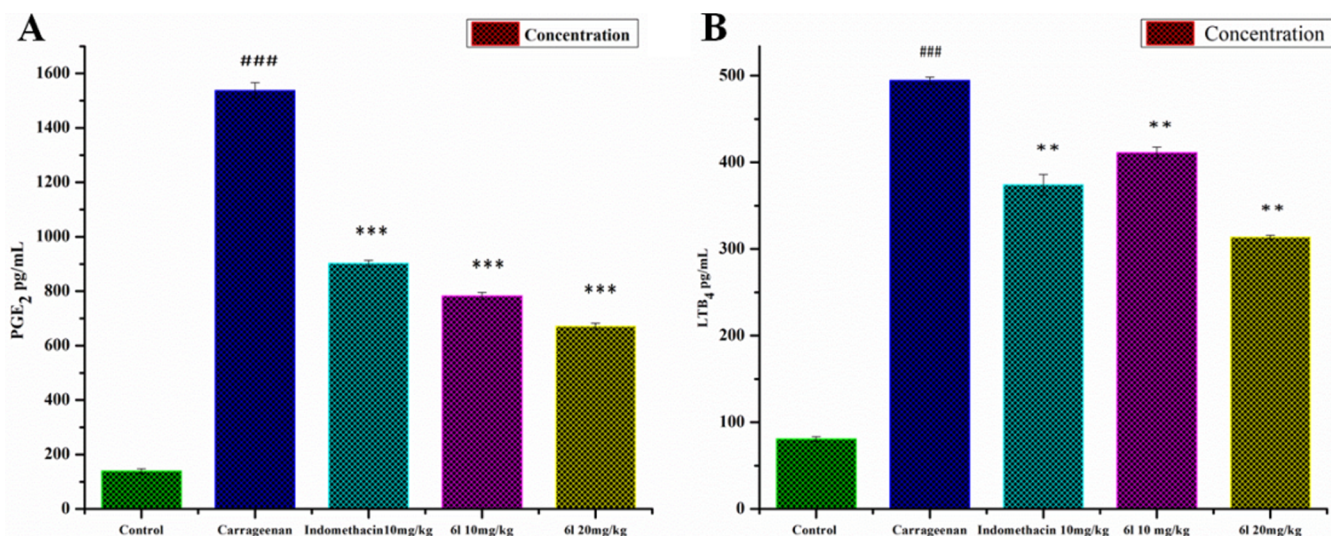


Fig. 6. Effects of compound **61** on PGE₂ and LTB₄ levels in paw tissues at 6 h after injection of carrageenan in the left hind paw. Animals were pre-treated with indomethacin and compound **61** 1 h before the carrageenan injection. The animals were sacrificed 6 h later and concentration of PGE₂ (Graph A) and LTB₄ (Graph B) was determined in the supernatant prepared from paws collected. Control group was treated only with saline. Pre-treatment was not given to carrageenan group. The values were expressed as the mean \pm SEM. ###p < 0.001 carrageenan group compared to control group. *p < 0.05, **p < 0.01, and ***p < 0.001 were compared with the carrageenan alone group.

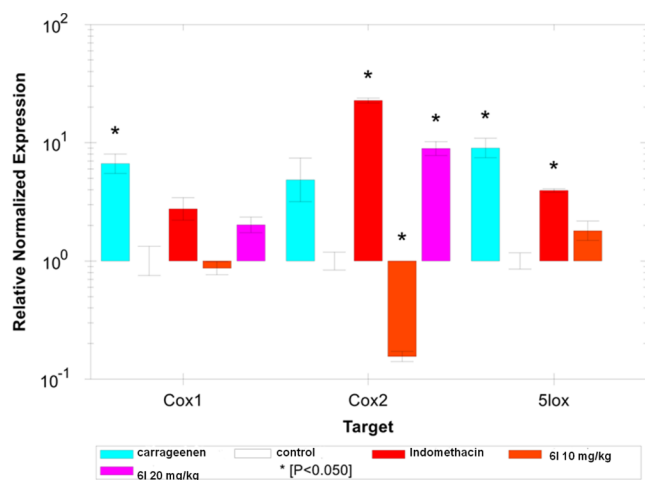


Fig. 7. Effect of compound **61** on COX-1, COX-2 and 5-LOX gene expression induced by carrageenan in the rat paw at 6 h. GAPDH was used as an internal control. Relative COX-1, COX-2 and 5-LOX gene expression was calculated at *p < 0.050. The values were expressed as the mean \pm SEM for experiments performed in triplicates.

2.7.4. Nitric oxide (NO) scavenging assay

In the NO scavenging assay, the synthesized compounds were able to forage NO moderately at 20 μ M concentration. Compound **6o** and **6h** showed the highest activity with $57.30 \pm 0.97\%$ and $54.23 \pm 0.75\%$ respectively. Compound **6l** showed $42.47 \pm 0.80\%$ NO scavenging activity which was similar to etoricoxib and 2 fold higher than indomethacin and ascorbic acid.

2.8. Molecular docking study

Experimental studies showed the potential of compound **6l** as a dual inhibitor of COX-2 and 5-LOX enzymes. To visualize the possible interactions of compound **6l** at COX-2 and 5-LOX active sites, molecular docking studies were performed using AutoDockTools-1.5.6 software. The compound **6l** proved the best binding pose in the COX-2 active site with binding energy -7.54 Kcal/mol. The oxygen atom of carbonyl group formed an H-bond with His351 amino acid residue. The diphenyl

amino group was residing in a hydrophobic pocket created by His90, Thr94, Pro514, Asp515, Pro191, Tyr355, Gly354, Gln192, and Ser 353 residues. The thiophenyl ring appeared in hydrophobic interaction with Ser581. Similarly, the 4-methyl phenyl ring was interacting and enclosed in a hydrophobic cavity created by His356 and Gln350. The larger volume of COX-2 active site accommodates the bulky aromatic rings of compound **6l** to attain the best binding conformation. Docking simulations afforded the binding interactions of compound **6l** and 5-LOX active site. Sulphur atoms of thiazole and thiophene ring of compound **6l** formed H bonds with Trp147 and Gln417 respectively. Binding energy of compound **6l** at 5-LOX active site was -6.99 Kcal/mol. While the reference drug zileuton showed a binding score of -6.43 Kcal/mol and two H bonds with Asn425 and Gln363. The **6l** molecule was surrounded by Ala157, Thr40, Asn148 and Glu412. The compound **6l** formed pi-sulfur interaction with Met145. Interactions of **6l** at COX-2 and 5-LOX are duly depicted in Fig. 9.

3. Conclusions

The present study described the green synthesis of thiazole and thiazolidene derivatives as potential dual COX-2/5-LOX inhibitors. Synthesized derivatives included 3 thioureas (**4a-c**), 13 substituted thiazoles (**6a-m**) and 5 substituted thiazolidenes (**6n-r**). These molecules were tested for both *in-vitro* and *in-vivo* anti-inflammatory assays. *In-vitro* assays demonstrated that the compound **6l** with diphenylamino group and 4-tolyl group on thiazole core was the most effective COX-2 and 5-LOX dual inhibitor with IC₅₀ values of 0.09 μ M and 0.38 μ M respectively. Interestingly, compound **6l** showed high selectivity towards COX-2 with a selectivity index of 61.66 which was comparable to that of etoricoxib which has SI of 91.28. Selected compounds showed a significant inhibition of PGE₂ and LTB₄ on LPS challenged RAW 264.7 cells. Meanwhile, *in-vivo* acute toxicity study was performed on rats and there was no evidence of toxicity. *In-vivo* anti-inflammatory assay results of compound **6l** showed significant reduction in edema in male Wistar rats (60.82%). Furthermore, the compound **6l** has better gastric safety profile than indomethacin on ulcerogenic potential screening. Histopathological examination of rat stomach treated with **6l** displayed a normal gastric mucosa with no ulceration. Subsequently, Rat paw tissues obtained followed to anti-inflammatory study, were subjected to qRT-PCR studies, PGE₂, and LTB₄ inhibitory studies. The qRT-PCR

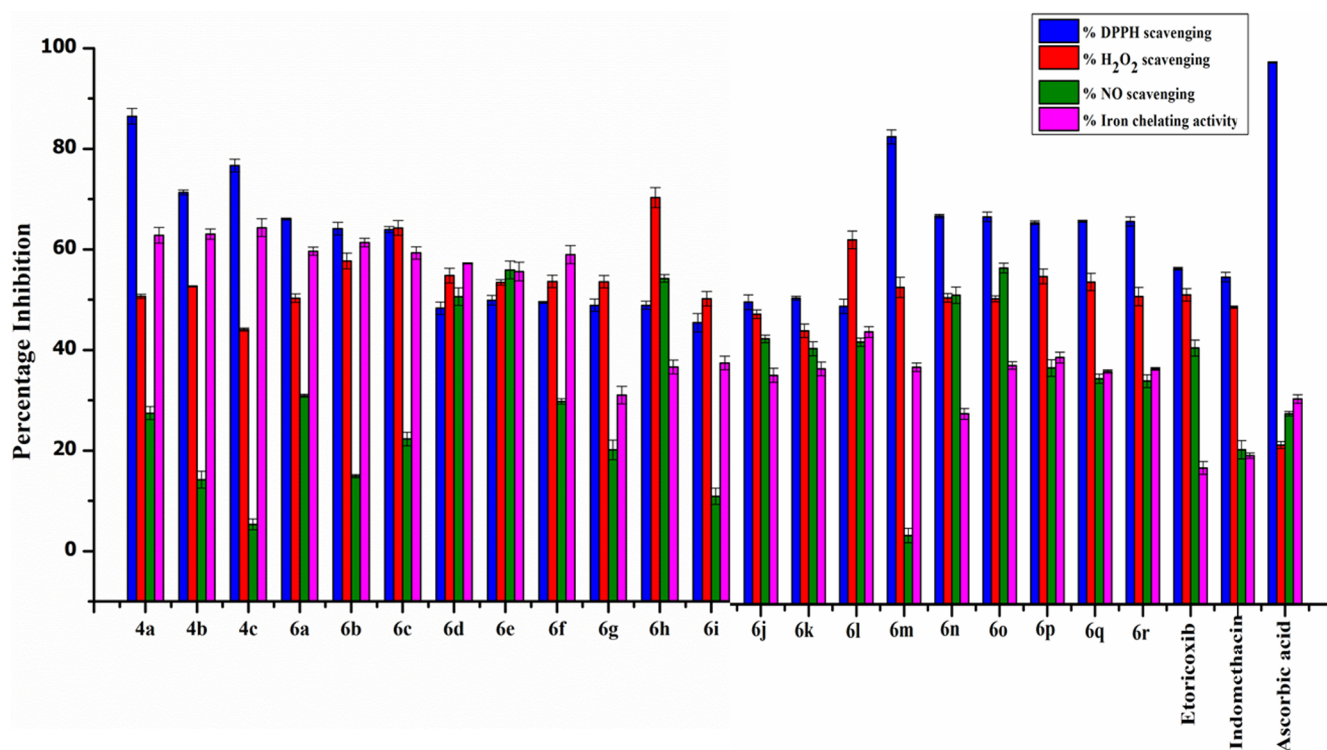


Fig. 8. Effect of synthesized compounds on DPPH scavenging, H₂O₂ scavenging, NO scavenging, and Iron chelating activity.

studies depicted a significant inhibition of **6l** on up-regulation of COX-2 and 5-LOX genes which was well matched with the obtained results. The compound **6l** significantly reduced the up-regulation of COX-2 and 5-LOX sparing its effect on COX-1. Similarly, PGE₂ and LTB₄ levels in the treated rat paws were very less compared to control. These stepwise investigations of *in-vitro*, *in-vivo* and qRT-PCR results indicated the discovery of a new ligand with high potency and selectivity against COX-2/5-LOX. The ligand **6l** could of course be further studied for the development of a potent anti-inflammatory drug with improved gastric safety profile.

4. Experimental section

4.1. Chemistry

All the chemicals were purchased from Sigma-Aldrich, Merck, TCI and Alfa Aesar and were used without further purification. Millipore water was used as a solvent for all reaction. Progression of the reaction was monitored by thin-layer chromatography on Merck silica gel 60 F254 pre-coated plates with ethyl acetate: hexane as mobile phase and visualization of the chromatogram was done by UV light and iodine chamber. Melting points were determined using the Guna melting point apparatus with open capillary tubes and were uncorrected. FTIR spectra of the synthesized compounds were recorded on (ATR-FTIR Jasco-4100) with DRS technology. ¹H and ¹³C NMR spectra were recorded on Bruker advance DMX 400 MHz NMR spectrometer using CDCl₃ and DMSO-*d*₆ containing internal standard tetramethylsilane (TMS). In NMR spectra, chemical shifts (δ) are expressed in parts per million (ppm) and coupling constants (J) are expressed in hertz (Hz). HRMS (High-resolution mass spectra) spectra were acquired using JOEL HR mass spectrometer. The chromatographic analysis was carried out by UPLC-PDA equipped with a pump quaternary solvent manager auto sampler- sample manager FTN, and PDA-E-LAMBDA detector. The used analytical column was Acquity UPLC BEH C 18 (150 mm × 2.1 mm i.d., 130 Å, 1.7 μm) at 37°C. The mobile phase was composed of 0.01 M Disodium phosphate and Methanol (10:50 v/v). Purity of all the tested

compounds was > 95%. The elemental analysis values were found to be within ± 0.4% of the calculated values (Perkin Elmer 2400 CHNS analyzer).

General method of preparation of compounds (**4a-c**, **6a-r**).

1.6 mmol of Potassium thiocyanate was added to a solution of 15 ml water and 0.1 equiv tetrabutylammonium fluoride (TBAF). To the above mixture, 1.5 mmol thiophene-2-carbonyl chloride was added and stirred for 30 min at RT. Further, 1.5 mmol Aromatic or alkyl amines were added and continued stirring until the reaction was completed (30–60 min), monitored by TLC (Compounds **4a-c** were separated at this stage). Then substituted phenacyl bromide (1.5 mmol) was added and refluxed with stirring at 80 °C for 2 h. The solid obtained was filtered and column chromatography was performed to achieve pure products (hexane:ethylacetate).

N-(morpholine-4-carbonothioyl)thiophene-2-carboxamide (**4a**). Off white solid, 89%, mp 162–164 °C. IR (KBr, cm⁻¹) 3278 (NH str), 2970 (aromatic C–H str), 1658 (amide C=O str), 1442 (aromatic C=C str), 1261 (morpholine C–N), 1111 (morpholine C–O–C), 731 (aromatic C–H bend). ¹H NMR (400 MHz, DMSO-*d*₆) δ: 3.57 (t, *J* = 26.2 Hz, 6H, morpholine-H), 4.15 (s, 2H, morpholine-H), 7.20 (t, *J* = 4.5 Hz, 1H, Thiophene-H), 7.91 (d, *J* = 4.9 Hz, 1H, Thiophene-H), 8.09 (d, *J* = 3.7 Hz, 1H, Thiophene-H), 10.89 (s, 1H, NH). ¹³C NMR (100 MHz, DMSO-*d*₆) δ: 50.9, 51.7, 66.1, 128.8, 131.7, 133.9, 138.2, 158.6, 179.5. ESI-MS *m/z* for C₁₀H₁₂N₂O₂S₂ [M + H]⁺ calcd 257.0340, found 257. Elemental analysis (%) calcd for C₁₀H₁₂N₂O₂S₂, C 46.86, H 4.72, N 10.93, S 25.01; found: C 46.54, H 4.37, N 10.71, S 25.07.

N-(diphenylcarbamothioyl)thiophene-2-carboxamide (**4b**). Yellow solid, 88%, mp 132–134 °C. IR (KBr, cm⁻¹) 3263 (NH str), 3070 (aromatic C–H str), 1672 (amide C=O str), 1485 (aromatic C=C str), 694 (aromatic C–H bend). ¹H NMR (400 MHz, CDCl₃) δ: 6.90 (t, *J* = 7.4 Hz, 1H, Thiophene-H), 7.02 (t, *J* = 4.8 Hz, 1H, Ar-H), 7.06 (d, *J* = 8.6 Hz, 2H, Ar-H), 7.24 (t, *J* = 6.0 Hz, 2H, Ar-H), 7.32–7.37 (m, 6H, Ar-H), 7.41 (d, *J* = 2.8 Hz, 1H, Ar-H), 7.51 (d, *J* = 4.9 Hz, 1H, Ar-H), 8.54 (s, 1H, Ar-H). ¹³C NMR (100 MHz, CDCl₃) δ: 117.8, 121.0, 126.9, 127.5, 127.9, 128.7, 129.3, 129.4, 130.3, 132.5, 135.8, 136.4, 143.2, 156.4, 181.5. ESI-MS *m/z* for C₁₈H₁₄N₂O₂S₂ [M + H]⁺ calcd

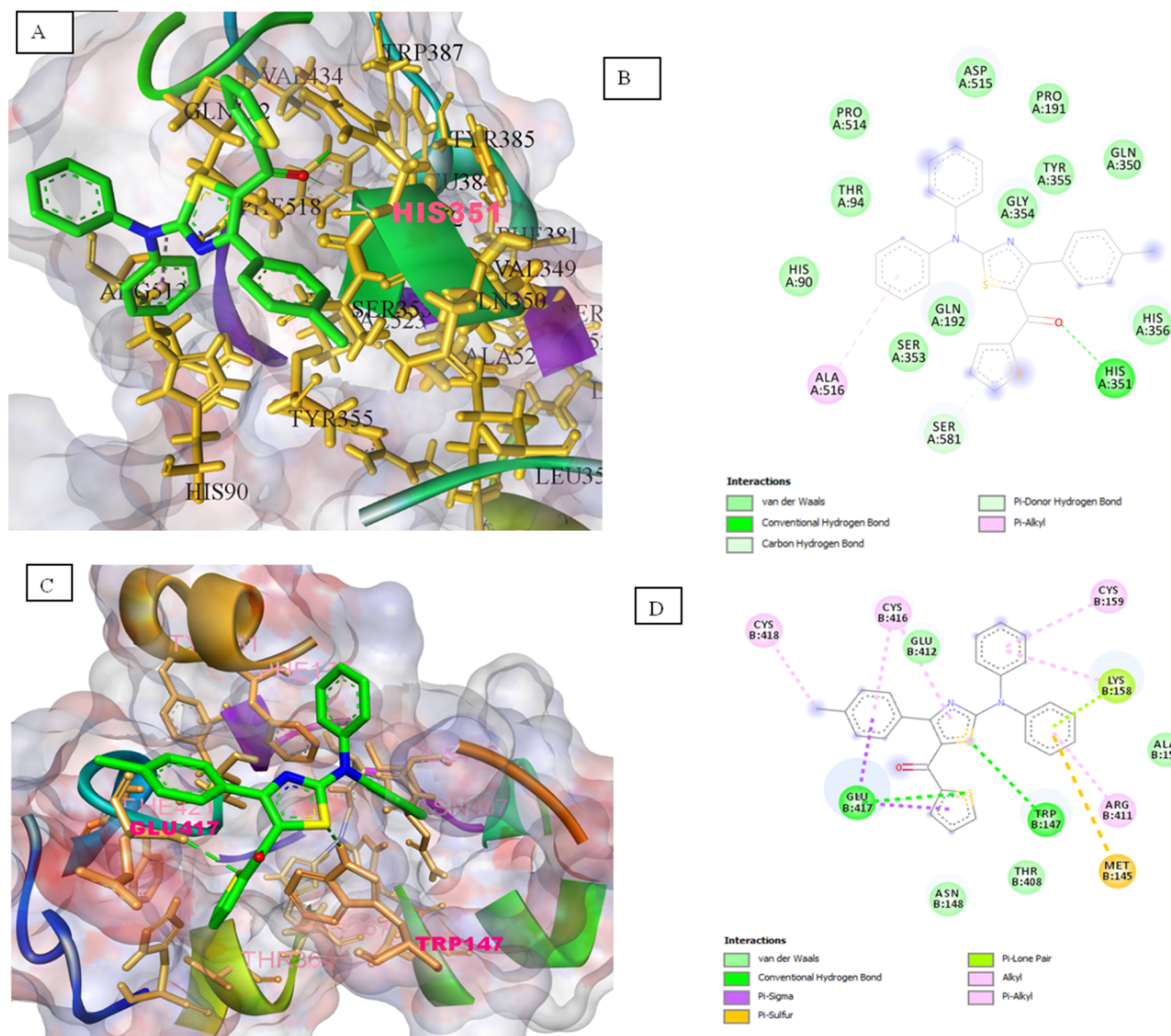


Fig. 9. Binding modes of compound **61** with amino acid residues of COX-2 (pdb ID 5IKT) and 5-LOX (pdb ID 3O8Y), (generated in Discovery Studio Visualizer) (A) Docked pose at COX-2 active site (B) 2-Dimensional representation at COX-2 active site (C) Docked pose at 5-LOX active site (D) 2-Dimensional representation at 5-LOX active site. Dashed green lines represent H-bonds. Colours depicted are Ligand: green, active site amino acid: orange, nitrogen: blue, oxygen: red, sulfur: yellow.

339.0548, found 339. Elemental analysis (%) calcd for $C_{18}H_{14}N_2O_2S_2$, C 63.88, H 4.17, N 8.28, S 18.95; found: C 63.62, H 4.20, N 8.62, S 19.04.

N-(phenylcarbamothioyl)thiophene-2-carboxamide (**4c**). Off White solid, 93%, mp 134–136 °C. IR (KBr, cm^{-1}) 3273 (NH str), 2964 (aromatic C–H str), 1658 (amide C=O str), 1483 (aromatic C=C str), 721 (aromatic C–H bend). 1H NMR (400 MHz, $CDCl_3$) δ : 7.18 (t, $J = 4.8$ Hz, 1H, Ar-H), 7.28 (d, $J = 7.5$ Hz, 1H, Ar-H), 7.40 (t, $J = 8.0$ Hz, 2H, Ar-H), 7.68 (d, $J = 7.8$ Hz, 2H, Ar-H), 7.72 (t, $J = 5.2$ Hz, 2H, Ar-H), 9.00 (s, 1H, NH), 12.39 (s, 1H, NH). ^{13}C NMR (100 MHz, $CDCl_3$) δ : 124.2, 126.9, 128.6, 128.9, 130.8, 134.4, 135.9, 137.6, 161.2, 178.1. ESI-MS m/z for $C_{12}H_{10}N_2O_2S_2$ $[M + H]^+$ calcd 263.0235, found 263. Elemental analysis (%) calcd for $C_{12}H_{10}N_2O_2S_2$, C 54.94, H 3.84, N 10.68, S 24.44; found: C 54.89, H 3.92, N 10.88, S 24.56.

(2-Morpholino-4-phenylthiazol-5-yl)(thiophen-2-yl)methanone (**6a**). Yellow solid, 91%, mp 124–126 °C. IR (KBr, cm^{-1}) 2991 (aromatic C–H str), 1732 (C=O str), 1610 (C=N str), 1490 (aromatic C=C str), 1417 (thiazole C–N), 1288 (morpholine C–N), 1112 (morpholine C–O–C), 694 (aromatic C–H bend), 638 (C–S str). 1H NMR (400 MHz,

$CDCl_3$) δ : 3.59 (t, $J = 4.7$ Hz, 4H, morpholine-H), 3.80 (t, $J = 5.2$ Hz, 4H, morpholine-H), 6.79 (t, $J = 3.9$ Hz, 1H, Thiophene-H), 7.28 (t, $J = 6.4$ Hz, 3H, Ar-H), 7.40 (d, $J = 7.4$ Hz, 1H, Ar-H), 7.44 (d, $J = 3.8$ Hz, 1H, Ar-H), 7.66 (d, $J = 7.1$ Hz, 2H, Ar-H). ^{13}C NMR (100 MHz, $CDCl_3$) δ : 48.0, 66.1, 119.9, 127.3, 128.1, 128.4, 128.8, 130.7, 131.8, 137.5, 139.6, 151.7, 170.8, 187.7. HRMS (ESI-MS) m/z for $C_{18}H_{16}N_2O_2S_2$ $[M + H]^+$ calcd 357.0653, found 357.0648. Elemental analysis (%) calcd for $C_{18}H_{16}N_2O_2S_2$, C 60.65, H 4.52, N 7.86, S 17.99; found: C 60.27, H 4.21, N 7.56, S 17.83.

(2-Morpholino-4-(4-nitrophenyl)thiazol-5-yl)(thiophen-2-yl)methanone (**6b**). Fluorescent yellow solid, 80%, mp 144–146 °C. IR (KBr, cm^{-1}) 3070 (aromatic C–H str), 1609 (C=O str), 1512 (NO₂ str), 1444 (aromatic C=C str), 1344 (thiazole C–N), 1298 (morpholine C–N), 1111 (morpholine C–O–C), 712 (aromatic C–H bend). 1H NMR (400 MHz, $CDCl_3$) δ : 3.63 (t, $J = 4.8$ Hz, 4H, morpholine-H), 3.84 (t, $J = 4.8$ Hz, 4H, morpholine-H), 6.87 (t, $J = 4.0$ Hz, 1H, Ar-H), 7.40 (d, $J = 3.2$ Hz, 1H, Ar-H), 7.55 (d, $J = 4.8$ Hz, 1H, Ar-H), 7.71 (d, $J = 8.4$ Hz, 2H, Ar-H), 8.10 (d, $J = 8.4$ Hz, 2H, Ar-H). ^{13}C NMR (100 MHz, $CDCl_3$) δ : 48.2, 66.0, 123.1, 127.6, 130.5, 133.7, 133.9,

141.4, 143.8, 147.6, 155.4, 178.8. HRMS (ESI-MS) m/z for $C_{18}H_{15}N_3O_4S_2$ [M + H]⁺ calcd 402.0504, found 402.0501. Elemental analysis (%) calcd for $C_{18}H_{15}N_3O_4S_2$, C 53.85, H 3.77, N 10.47, S 15.97; found: C 53.57, H 3.43, N 9.99, S 16.0.

(4-(4-Fluorophenyl)-2-morpholinothiazol-5-yl)(thiophen-2-yl)methanone (**6c**). Yellow solid, 86%, mp 110–112 °C. IR (KBr, cm^{-1}) 2962 (aromatic C–H str), 1614 (C=O str), 1595 (C=N str), 1442 (aromatic C=C str), 1365 (thiazole C–N), 1259 (morpholine C–N), 1111 (morpholine C–O–C), 1029 (C–F str), 719 (aromatic C–H bend), 646 (C–S str). ¹H NMR (400 MHz, $CDCl_3$) δ : 3.60 (t, J = 3.9 Hz, 4H, morpholine-H), 3.81 (t, J = 4.3 Hz, 4H, morpholine-H), 6.80 (t, J = 4.2 Hz, 1H, Ar-H), 6.94 (t, J = 8.2 Hz, 2H, Ar-H), 7.29 (d, J = 5.2 Hz, 2H, Ar-H), 7.67 (t, J = 6.0 Hz, 2H, Ar-H). ¹³C NMR (100 MHz, $CDCl_3$) δ : 48.0, 66.1, 115.1, 115.3, 119.9, 127.3, 128.5, 130.8, 131.4, 131.5, 131.6, 135.5, 135.6, 137.2, 151.7, 163.6, 166.1, 170.9, 186.4. HRMS (ESI-MS) m/z for $C_{18}H_{15}FN_2O_2S_2$ [M + H]⁺ calcd 375.0559, found 375.0552. Elemental analysis (%) calcd for $C_{18}H_{15}FN_2O_2S_2$, C 57.74, H 4.04, N 7.48; S 17.12 found: C 57.76, H 4.02, N 7.83, S 17.02.

(2-Morpholino-4-(4-(trifluoromethyl)phenyl)thiazol-5-yl)(thiophen-2-yl)methanone (**6d**). Yellow solid, 84%, mp 92–94 °C. IR (KBr, cm^{-1}) 3076 (aromatic C–H str), 1718 (C=O str), 1508 (C=N str) 1473 (aromatic C=C str), 1327 (thiazole C–N), 1228 (morpholine C–N), 1099 (morpholine C–O–C), 804 (aromatic CH bend), 630 (C–S str). ¹H NMR (400 MHz, $CDCl_3$) δ : 3.62 (t, J = 4.6 Hz, 4H, morpholine-H), 3.83 (t, J = 5.1 Hz, 4H, morpholine-H), 6.83 (t, J = 4.7 Hz, 1H, Ar-H), 7.32 (d, J = 3.0 Hz, 1H, Ar-H), 7.48 (t, J = 8.2 Hz, 3H, Ar-H), 7.63 (d, J = 8.1 Hz, 2H, Ar-H). ¹³C NMR (100 MHz, $CDCl_3$) δ : 48.2, 66.1, 121.2, 124.9, 124.9, 127.5, 129.9, 133.6, 138.6, 143.7, 156.6, 171.4, 179.1. HRMS (ESI-MS) m/z for $C_{19}H_{15}F_3N_2O_2S_2$ [M + H]⁺ calcd 425.0527, found 425.0524. Elemental analysis (%) calcd for $C_{19}H_{15}F_3N_2O_2S_2$, C 53.77, H 3.56, N 6.60, S 15.11 found: C 53.77, H 3.67, N 6.62, S 15.19.

4-(2-Morpholino-5-(thiophene-2-carbonyl)thiazol-4-yl)benzotrile (**6e**). Bright yellow solid, 89%, mp 158–160 °C. IR (KBr, cm^{-1}) 2984 (aromatic C–H str), 2218 (CN str), 1598 (C=O str), 1510 (C=N str) 1473 (aromatic C=C str), 1413 (thiazole C–N), 1292 (morpholine C–N), 1111 (morpholine C–O–C), 794 (aromatic C–H bend), 642 (C–S str). ¹H NMR (400 MHz, $CDCl_3$) δ : 3.63 (t, J = 4.6 Hz, 4H, morpholine-H), 3.82 (t, J = 5.2 Hz, 4H, morpholine-H), 6.76 (t, J = 5.0 Hz, 1H, Ar-H), 7.27 (d, J = 2.9 Hz, 1H, Ar-H), 7.32 (d, J = 5.0 Hz, 1H, Ar-H), 7.54 (d, J = 8.4 Hz, 2H, Ar-H), 7.66 (d, J = 8.4 Hz, 2H, Ar-H). ¹³C NMR (100 MHz, $CDCl_3$) δ : 48.1, 66.0, 114.6, 118.1, 120.0, 127.3, 129.1, 129.2, 131.3, 131.8, 136.8, 143.3, 153.1, 171.4, 185.8. HRMS (ESI-MS) m/z for $C_{19}H_{15}N_3O_2S_2$ [M + H]⁺ calcd 382.0606, found 382.0603. Elemental analysis (%) calcd for $C_{19}H_{15}N_3O_2S_2$, C 59.82, H 3.96 N 11.02, S 16.81; found: C 59.89, H 3.96, N 11.02, S 15.91.

(2-Morpholino-4-(*p*-tolyl)thiazol-5-yl)(thiophen-2-yl)methanone (**6f**). Pale yellow solid, 81%, mp 106–108 °C. IR (KBr, cm^{-1}) 2978 (aromatic C–H str), 2856 (C–CH₃ str), 1597 (C=O str), 1508 (aromatic C=C str), 1481 (thiazole C–N), 1286 (morpholine C–N), 1112 (morpholine C–O–C), 786 (aromatic C–H bend), 651 (C–S str). ¹H NMR (400 MHz, $CDCl_3$) δ : 2.28 (s, 3H, CH₃), 3.61 (t, J = 4.7 Hz, 4H, morpholine-H), 3.81 (t, J = 5.1 Hz, 4H, morpholine-H), 6.77 (t, J = 4.9 Hz, 1H, Ar-H), 7.01 (d, J = 7.9 Hz, 2H, Ar-H), 7.24 (d, J = 4.8 Hz, 1H, Ar-H), 7.39 (d, J = 8.1 Hz, 2H, Ar-H), 7.44 (d, J = 5.9 Hz, 1H, Ar-H). ¹³C NMR (100 MHz, $CDCl_3$) δ : 21.4, 48.1, 66.1, 120.4, 127.3, 128.7, 129.6, 132.7, 133.5, 138.9, 143.8, 158.3, 171.2, 179.7. HRMS (ESI-MS) m/z for $C_{19}H_{18}N_2O_2S_2$ [M + H]⁺ calcd 371.0810, found 371.0807. Elemental analysis (%) calcd for $C_{19}H_{18}N_2O_2S_2$, C 61.60, H 4.90, N 7.56, S 17.31; found: C 60.98, H 4.89, N 7.39, S 17.29.

(2-(Diphenylamino)-4-phenylthiazol-5-yl)(thiophen-2-yl)methanone (**6g**). Pale yellow solid, 86%, mp 201–204 °C. IR (KBr, cm^{-1}) 3076 (aromatic C–H str), 1597 (C=O str), 1490 (aromatic C=C str), 1332 (thiazole C–N), 792 (aromatic C–H bend), 690 (C–S str). ¹H NMR (400 MHz, $DMSO-d_6$) δ : 6.91 (t, J = 4.0 Hz, 1H, Ar-H), 7.26 (d, J = 6.2, 2H, Ar-H), 7.34 (t, J = 6.9, 3H, Ar-H), 7.41 (d, J = 7.9 Hz, 2H, Ar-H),

7.48 (t, J = 8.1 Hz, 5H, Ar-H), 7.56 (d, J = 8.1 Hz, 4H, Ar-H), 7.86 (d, J = 4.9 Hz, 1H, Ar-H). ¹³C NMR (100 MHz, $CDCl_3$) δ : 122.5, 126.1, 126.8, 127.4, 127.9, 128.8, 133.2, 133.9, 134.9, 143.7, 144.2, 156.9, 169.8, 180.0. HRMS (ESI-MS) m/z for $C_{26}H_{18}N_2OS_2$ [M + H]⁺ calcd 439.0861, found 439.0855. Elemental analysis (%) calcd for $C_{26}H_{18}N_2OS_2$, C 71.21, H 4.14, N 6.39, S 14.62; found: C 70.90, H 4.60, N 6.79, S 14.39.

(2-(Diphenylamino)-4-(4-nitrophenyl)thiazol-5-yl)(thiophen-2-yl)methanone (**6h**). Fluorescent yellow solid, 92%, mp 158–160 °C. IR (KBr, cm^{-1}) 3076 (aromatic C–H str), 1604 (C=O str), 1510 (aromatic C=C str), 1340 (thiazole C–N), 788 (aromatic C–H bend), 698 (C–S str). ¹H NMR (400 MHz, $CDCl_3$) δ : 6.87 (t, J = 4.8 Hz, 1H, Ar-H), 7.30 (t, J = 6.7 Hz, 2H, Ar-H), 7.44–7.48 (m, 9H, Ar-H), 7.55 (d, J = 4.9, 1H, Ar-H), 7.71 (d, J = 8.8, 2H, Ar-H), 8.08 (d, J = 8.1 Hz, 2H, Ar-H). ¹³C NMR (100 MHz, $CDCl_3$) δ : 123.2, 126.1, 127.2, 127.8, 129.9, 130.5, 134.1, 141.1, 143.8, 144.0, 147.5, 154.2, 170.0, 179.1. HRMS (ESI-MS) m/z for $C_{26}H_{17}N_3O_3S_2$ [M + H]⁺ calcd 484.0711, found 484.0706. Elemental analysis (%) calcd for $C_{26}H_{17}N_3O_3S_2$, C 64.58, H 3.54, N 8.69, S 13.26; found: C 64.15, H 3.58, N 8.59, S 13.30.

(2-(Diphenylamino)-4-(4-fluorophenyl)thiazol-5-yl)(thiophen-2-yl)methanone (**6i**). Yellow solid, 86%, mp 130–132 °C. IR (KBr, cm^{-1}), 3061 (aromatic C–H str), 1608 (C=O str), 1442 (aromatic C=C str), 1332 (thiazole C–N), 1151 (C–F str) 750 (aromatic C–H bend), 684 (C–S str). ¹H NMR (400 MHz, $CDCl_3$) δ : 6.82 (t, J = 4.8 Hz, 1H, Ar-H), 6.88 (t, J = 8.8 Hz, 2H, Ar-H), 7.28–7.32 (m, 3H, Ar-H), 7.41–7.50 (m, 9H, Ar-H), 7.51–7.55 (m, 2H, Ar-H). ¹³C NMR (100 MHz, $CDCl_3$) δ : 114.9, 115.1, 122.0, 126.2, 126.9, 127.5, 129.8, 131.1, 131.1, 131.6, 131.7, 133.4, 133.9, 143.8, 144.2, 155.9, 161.8, 164.2, 169.9, 179.7. HRMS (ESI-MS) m/z for $C_{26}H_{17}FN_2OS_2$ [M + H]⁺ calcd 457.0766, found 457.0761. Elemental analysis (%) calcd for $C_{26}H_{17}FN_2OS_2$, C 68.40, H 3.75, N 6.14, S, 14.04; found: C 68.38, H 3.92, N 6.29, S 14.32.

(2-(Diphenylamino)-4-(4-(trifluoromethyl)phenyl)thiazol-5-yl)(thiophen-2-yl)methanone (**6j**). Yellow solid, 88%, mp 128–130 °C. IR (KBr, cm^{-1}) 3062 (aromatic C–H str), 1598 (C=O str), 1498 (aromatic C=C str), 1317 (thiazole C–N), 754 (aromatic C–H bend), 690 (C–S str). ¹H NMR (400 MHz, $CDCl_3$) δ : 6.84 (t, J = 4.1 Hz, 1H, Ar-H), 7.29 (t, J = 7.0 Hz, 2H, Ar-H), 7.36 (d, J = 3.0 Hz, 1H, Ar-H), 7.42 (m, 11H, Ar-H), 7.71 (d, J = 8.0 Hz, 1H, Ar-H), 8.08 (d, J = 8.2 Hz, 1H, Ar-H). ¹³C NMR (100 MHz, $CDCl_3$) δ : 122.7, 124.8, 124.9, 124.9, 126.1, 127.1, 127.6, 129.9, 130.3, 130.6, 133.8, 134.0, 138.4, 143.8, 144.1, 155.4, 170.0, 179.4. HRMS (ESI-MS) m/z for $C_{27}H_{17}F_3N_2OS_2$ [M + H]⁺ calcd 507.0734, found 507.0731. Elemental analysis (%) calcd for $C_{27}H_{17}F_3N_2OS_2$, C 64.02, H 3.38, N 5.53, S, 12.66; found: C 64.05, H 3.57, N 5.50, S 12.69.

4-(2-(Diphenylamino)-5-(thiophene-2-carbonyl)thiazol-4-yl)benzotrile (**6k**). Yellow solid, 85%, mp 188–190 °C. IR (KBr, cm^{-1}) 3095 (aromatic C–H str), 2222 (CN str), 1600 (C=O str), 1487 (aromatic C=C str), 1338 (thiazole C–N), 758 (aromatic C–H bend), 699 (C–S str). ¹H NMR (400 MHz, $DMSO-d_6$) δ : 6.99 (t, J = 4.2 Hz, 1H, Ar-H), 7.35 (t, J = 7.2 Hz, 2H, Ar-H), 7.46 (d, J = 3.7 Hz, 1H, Ar-H), 7.48 (t, J = 8.0, 4H, Ar-H), 7.56 (d, J = 7.9, 4H, Ar-H), 7.61 (d, J = 8.3, 2H, Ar-H), 7.74 (d, J = 8.2 Hz, 2H, Ar-H), 7.93 (d, J = 4.9 Hz, 1H, Ar-H). ¹³C NMR (100 MHz, $DMSO-d_6$) δ : 111.6, 119.0, 122.4, 126.9, 127.9, 128.7, 130.5, 130.6, 132.4, 135.0, 135.8, 139.5, 143.5, 144.2, 155.0, 170.1, 178.7. HRMS (ESI-MS) m/z for $C_{27}H_{17}N_3OS_2$ [M + H]⁺ calcd 464.0813, found 464.0811. Elemental analysis (%) calcd for $C_{27}H_{17}N_3OS_2$, C 69.96, H 3.70, N 9.06, S 13.83; found: C 69.61, H 4.00, N 9.59, S 14.48.

(2-(Diphenylamino)-4-(*p*-tolyl)thiazol-5-yl)(thiophen-2-yl)methanone (**6l**). Yellow solid, 86%, mp 142–144 °C. IR (KBr, cm^{-1}) 3059 (aromatic C–H str), 1583 (C=O str), 1446 (aromatic C=C str), 1328 (thiazole C–N), 736 (aromatic C–H bend), 692 (C–S str). ¹H NMR (400 MHz, $CDCl_3$) δ : 2.33 (s, 3H, CH₃), 6.83 (t, J = 3.9 Hz, 1H, Thiophene-H), 7.09 (d, J = 8.0 Hz, 2H, Ar-H), 7.25–7.29 (m, 3H, Ar-H), 7.39–7.47 (m, 8H, Ar-H), 7.49 (d, J = 3.8 Hz, 1H, Ar-H), 7.62 (d, J = 8.0 Hz, 2H, Ar-H). ¹³C NMR (100 MHz, $CDCl_3$) δ : 21.6, 120.8, 126.1, 126.8, 127.3, 128.2,

128.9, 129.2, 129.7, 130.2, 136.7, 137.7, 142.9, 144.0, 150.4, 169.1, 187.6. HRMS (ESI-MS) m/z for $C_{27}H_{20}N_2OS_2$ $[M + H]^+$ calcd 453.1017, found 453.1013. Elemental analysis (%) calcd for $C_{27}H_{20}N_2OS_2$, C 71.65, H 4.45, N 6.19, S 14.17; found: C 71.62, H 4.84, N 5.98, S 14.29.

(4-(4-Fluorophenyl)-2-(phenylamino)thiazol-5-yl)(thiophen-2-yl)methanone (**6m**). Off white solid, 78%, mp 120–122 °C. IR (KBr, cm^{-1}) 3277 (N–H str), 3074 (aromatic C–H str), 1660 (C=O str), 1408 (aromatic C=C str), 1354 (thiazole C–N), 1141 (C–F str) 723 (aromatic C–H bend) 646 (C–S str). 1H NMR (400 MHz, DMSO $_d$) δ : 6.98 (t, $J = 4.2$ Hz, 1H, Ar-H), 7.05 (t, $J = 8.7$, 1H, Ar-H), 7.13 (t, $J = 8.8$, 2H, Ar-H), 7.37 (t, $J = 8.1$, 2H, Ar-H), 7.44 (d, $J = 3.7$ Hz, 1H, Ar-H), 7.57 (t, $J = 5.6$ Hz, 2H, Ar-H), 7.67 (d, $J = 7.9$ Hz, 2H, Ar-H), 7.91 (d, $J = 4.8$ Hz, 1H, Ar-H), 10.91 (s, 1H, NH). ^{13}C NMR (100 MHz, DMSO $_d$) δ : 115.3, 115.5, 115.9, 118.6, 119.4, 123.3, 128.5, 129.7, 131.7, 131.8, 132.0, 132.1, 134.7, 135.1, 140.5, 143.7, 155.8, 161.5, 163.9, 165.2, 179.3. HRMS (ESI-MS) m/z for $C_{20}H_{13}FN_2OS_2$ $[M + H]^+$ calcd 381.0453, found 381.0448. Elemental analysis (%) calcd for $C_{20}H_{13}FN_2OS_2$, C 66.27, H 3.89, N 7.73, S 17.69; found: C 67.19, H 3.51, 7.38, S 17.88.

N-(3,4-diphenylthiazol-2(3H)-ylidene)thiophene-2-carboxamide (**6n**). Off white solid, 85%, mp 198–200 °C. IR (KBr, cm^{-1}) 3100 (aromatic C–H str), 1576 (C=O str), 1467 (aromatic C=C str), 1364 (thiazole C–N), 754 (aromatic C–H bend) 691 (C–S str). 1H NMR (400 MHz, DMSO $_d$) δ : 7.06 (t, $J = 3.7$ Hz, 1H, Ar-H), 7.20–7.23 (m, 3H, Ar-H), 7.25–7.30 (m, 3H, Ar-H), 7.33–7.36 (m, 2H, Ar-H), 7.40–7.45 (m, 3H, Ar-H), 7.52 (d, $J = 4.8$ Hz, 1H, Ar-H), 7.66 (d, $J = 6.1$ Hz, 1H, Ar-H). ^{13}C NMR (100 MHz, DMSO $_d$) δ : 108.4, 128.4, 128.7, 129.2, 129.2, 129.3, 129.5, 130.7, 131.1, 132.3, 137.7, 139.1, 143.2, 168.7, 169.0. HRMS (ESI-MS) m/z for $C_{20}H_{14}N_2OS_2$ $[M + H]^+$ calcd 363.0548, found 363.0545. Elemental analysis (%) calcd for $C_{20}H_{14}N_2OS_2$, C 58.96, H 3.22, N 10.31, S 15.74; found: C 59.19, H 3.12, N 10.64, S 15.55.

N-(4-(4-nitrophenyl)-3-phenylthiazol-2(3H)-ylidene)thiophene-2-carboxamide (**6o**). Yellow solid, 87%, mp 248–250 °C. IR (KBr, cm^{-1}) 3110 (aromatic C–H str), 1605 (C=O str), 1460 (aromatic C=C str), 1362 (thiazole C–N), 748 (aromatic C–H bend), 697 (C–S str). 1H NMR (400 MHz, DMSO $_d$) δ : 7.08 (t, $J = 4.9$, 1H, Ar-H), 7.40–7.42 (m, 2H, Ar-H), 7.44–7.51 (m, 6H, Ar-H), 7.55 (d, $J = 3.6$ Hz, 1H, Ar-H), 7.69 (d, $J = 3.7$ Hz, 1H, Ar-H), 8.12 (d, $J = 8.8$ Hz, 2H, Ar-H). ^{13}C NMR (100 MHz, DMSO $_d$) δ : 111.2, 123.8, 128.5, 129.1, 129.4, 130.7, 131.3, 132.6, 137.0, 137.0, 137.4, 142.9, 147.7, 168.8, 169.1. HRMS (ESI-MS) m/z for $C_{20}H_{13}N_3O_3S_2$ $[M + H]^+$ calcd 408.0398, found 408.0391. Elemental analysis (%) calcd for $C_{20}H_{13}N_3O_3S_2$, C 63.14, H 3.44, N 7.36, S 16.85; found: C 63.34, H 3.61, N 7.30, S 16.78.

N-(3-phenyl-4-(4-(trifluoromethyl)phenyl)thiazol-2(3H)-ylidene)thiophene-2-carboxamide (**6p**). Off white solid, 86%, mp 228–230 °C. IR (KBr, cm^{-1}) 3107 (aromatic C–H str), 1576 (C=O str), 1464 (aromatic C=C str), 1322 (thiazole C–N), 759 (aromatic C–H bend), 689 (C–S str). 1H NMR (400 MHz, DMSO $_d$) δ : 7.08 (t, $J = 4.9$ Hz, 1H, Ar-H), 7.38–7.41 (m, 3H, Ar-H), 7.43–7.47 (m, 5H, Ar-H), 7.54 (d, $J = 2.4$ Hz, 1H, Ar-H), 7.65 (s, 1H, Ar-H), 7.68–7.69 (m, 2H, Ar-H). ^{13}C NMR (100 MHz, DMSO $_d$) δ : 110.1, 123.0, 125.6, 125.66, 125.7, 128.5, 129.1, 129.3, 129.3, 129.6, 130.3, 131.3, 132.5, 134.8, 137.4, 137.5, 143.0, 168.8, 169.1. HRMS (ESI-MS) m/z for $C_{21}H_{13}F_3N_2OS_2$ $[M + H]^+$ calcd 431.0421, found 431.0416. Elemental analysis (%) calcd for $C_{21}H_{13}F_3N_2OS_2$, C 58.60, H 3.04, N 6.51, S 14.90 found: C 58.66, H 3.13, N 6.87, S 13.98.

N-(4-(4-cyanophenyl)-3-phenylthiazol-2(3H)-ylidene)thiophene-2-carboxamide (**6q**). Pale yellow solid, 88%, mp 260–262 °C. IR (KBr, cm^{-1}) 3108 (aromatic C–H str), 2227 (CN str), 1575 (C=O str), 1447 (aromatic C=C str), 1362 (thiazole C–N), 754 (aromatic C–H bend), 693 (C–S str). 1H NMR (400 MHz, DMSO $_d$) δ : 7.07 (t, $J = 4.0$ Hz, 1H, Ar-H), 7.37–7.42 (m, 5H, Ar-H), 7.43–7.48 (m, 3H, Ar-H), 7.54 (d, $J = 3.6$, 1H, Ar-H), 7.67 (d, $J = 4.9$ Hz, 1H, Ar-H), 7.75 (d, $J = 8.2$ Hz, 2H, Ar-H). ^{13}C NMR (100 MHz, DMSO $_d$) δ : 110.6, 111.8, 118.7, 128.5, 129.1, 129.4, 129.4, 130.3, 131.3, 132.5, 132.6, 135.2, 137.4, 142.9,

168.8, 169.1. HRMS (ESI-MS) m/z for $C_{21}H_{13}N_3OS_2$ $[M + H]^+$ calcd 388.0500 found 388.0492. Elemental analysis (%) calcd for $C_{21}H_{13}N_3OS_2$, C 65.10, H 3.38, N 10.84, S 16.55; found: C 65.20, H 3.42, N 10.64, S 16.62.

N-(3-phenyl-4-(*p*-tolyl)thiazol-2(3H)-ylidene)thiophene-2-carboxamide (**6r**). Pale yellow solid, 84%, mp 208–210 °C. IR (KBr, cm^{-1}) 3108 (aromatic C–H str), 1583 (C=O str), 1468 (aromatic C=C str), 1366 (thiazole C–N), 741 (aromatic C–H bend), 699 (C–S str). 1H NMR (400 MHz, DMSO $_d$) δ : 2.24 (s, 3H, CH $_3$), 7.06–7.11 (m, 5H, Ar-H) 7.15 (s, 1H, Ar-H), 7.32 (d, $J = 6.64$ Hz, 2H, Ar-H), 7.41–7.46 (m, 3H, Ar-H), 7.51 (d, $J = 3.6$ Hz, 1H, Ar-H), 7.65 (d, $J = 4.9$ Hz, 1H, Ar-H). ^{13}C NMR (100 MHz, DMSO $_d$) δ : 21.2, 107.8, 127.8, 128.4, 129.1, 129.2, 129.3, 129.4, 131.1, 132.3, 137.8, 138.9, 139.1, 143.2, 168.7, 169.1. HRMS (ESI-MS) m/z for $C_{21}H_{16}N_2OS_2$ $[M + H]^+$ calcd 377.0704, found 377.0701. Elemental analysis (%) calcd for $C_{21}H_{16}N_2OS_2$, C 67.00, H 4.28, N 7.44, S, 17.03; found: C 67.02, H 4.03, N 7.25, S 17.09.

4.2. Biological activity

4.2.1. In-vitro COX-1 and COX-2 enzyme inhibition assay

COX-1 and COX-2 enzyme inhibition were screened by COX-1 (human) inhibitor screening assay kit (Catalogue no. 701070 Cayman chemical, USA) and COX-2 (human) inhibitory screening assay kit (Catalogue no. 701,080 Cayman chemical, USA) according to manufacturer's instructions. Briefly, SnCl $_2$ reduces COX derived PGH $_2$ produced during the COX reaction to PGF $_{2\alpha}$ and was measured directly. 100% initial activity tubes of enzyme were prepared by the addition of 160 μ l reaction buffer (0.1 M Tris-HCl of pH 8.0, containing 2 mM phenol and 5 mM EDTA), 10 μ l Heme and 10 μ l COX-1/COX-2 enzymes into particular tubes. Similarly, COX-1 and COX-2 inhibitor tubes were prepared by adding 10 μ l of inhibitor besides above components in each tube. Background tubes consist of inactivated enzymes obtained by placing the enzyme tubes in boiling water for 3 min. Then tubes were incubated at 37 °C for 10 min and addition of 10 μ l of arachidonic acid initiated the reaction in every tube followed by incubation for exactly 2 min at 37 °C. Enzyme catalysis was stopped by the addition of 30 μ l of stannous chloride. PGs produced in each reaction tube were quantified by ELISA method. All the compounds were screened against COX-2 at 0.01, 0.1, 1.0, 10.0 and 100.0 μ M in duplicate and percentage inhibition was determined. Compounds with promising activity were further studied against COX-1 at 0.1, 1.0, and 10.0 μ M in duplicate and IC $_{50}$ values were determined from dose-response curve [1].

4.2.2. In-vitro 5-LOX inhibitory assay

5-LOX enzyme inhibition was studied by Lipoxygenase inhibitor screening assay kit (Catalogue no. 760700 Cayman chemical, USA) together with 5-lipoxygenase (potato) screening enzyme (Catalogue no.60401, Cayman chemical, USA) according to manufacturer's instructions. Briefly, blank (100 μ l assay buffer), positive control wells (90 μ l of 5-LOX enzyme and 10 μ l assay buffer) 100% initial activity wells (90 μ l 5-LOX enzyme and 10 μ l inhibitor vehicle) and inhibitor wells (90 μ l 5-LOX enzyme and 10 μ l inhibitor) were incubated for 5 min at RT. 10 μ l linoleic acid was added to initiate the reaction. After incubation, addition of 100 μ l chromogen stopped enzyme catalysis and developed the reaction. The plate was shaken for 5 min and absorbance was read at 495 nm using the 96 well plate reader. All compounds were screened at 0.1, 1.0 and 10.0 μ M in duplicate and determined IC $_{50}$ values [1].

4.2.3. Measurement of PGE $_2$ and LTB $_4$ levels in LPS- stimulated RAW 264.7 cells

To investigate the anti-inflammatory effect of compounds, the production of PGE $_2$ and LTB $_4$ in LPS- stimulated RAW 264.7 cells were examined. Briefly, RAW 264.7 cells were seeded on 96 well plate at a density of 1×10^4 cells per well and incubated for 18 h. Cells were pre-treated with aspirin (500 μ M) for 3 h to inactivate the effect of COX-1

(endogenous cyclooxygenase-1). Then cells were washed with PBS (phosphate buffered saline) twice. Cells were subsequently pre-treated with various concentrations of test compounds, etoricoxib, and zileuton (0.1, 1.0, 10.0 μM) for 2 h before further incubation for 16 h in fresh Dulbecco's Modified Eagles medium (DMEM) with or without LPS (1 $\mu\text{g}/\text{ml}$). After incubation, supernatant was collected by centrifugation. [36] PGE₂ and LTB₄ levels were measured by ELISA technique using prostaglandin E₂ and leukotriene B₄ parameter Kits according to manufacturer's instruction. (Catalogue No. KGE004B & KGE006B, R&D Systems, Inc. USA).

4.2.4. In-vivo biological studies

Acute toxicity, *in-vivo* anti-inflammatory, and gastric safety profiling were performed using male Wistar rats. Animals were maintained at 23 \pm 2 °C in 12 h light/dark cycles with free access to water and food in the animal house, Vellore Institute of Technology, Vellore, Tamil Nadu. All the experimental procedures have been duly approved by CPSCEA (Committee for the Purpose of Control and Supervision of Experiments on Animals) Institutional Animal Ethics Committee (Approval no. VIT/IEAC/14/Nov5/35).

4.2.5. Studies for checking toxicity

Compound **61** was studied for its acute toxicity effect on Wistar rats as per OECD recommendations. Briefly, the animals were separated into four sets each consisting of three animals. Animals were fasted overnight before treatment with water ad libitum and 4 h after the treatment. Group I was control received vehicle, and compound **61** at 50 mg/kg, 500 mg/kg and 2000 mg/kg were administered orally to Group II, III and IV respectively in a single dose. In the first 4 h, animals were continuously monitored and then periodically for 24 h. Animals were sacrificed after 14 days and gross assessment of kidney, liver, stomach, and intestine was performed by histopathological studies of paraffin-embedded samples stained with hematoxylin and eosin [37].

4.2.6. Anti-inflammatory studies and gastric safety profiling

Male Wistar rats weighing 150–180 g were subjected to gastric safety profiling and carrageenan induced rat paw edema studies subsequently on the same set of rats. The ulcerogenic potential of compound **61** was studied according to Ganguly and Bhatnagar [38] with minor modification. Animals were grouped to five sets, comprising five animals each. Group I, control, consists of animals treated with vehicle. Indomethacin 10 mg/kg was administered to Group II. Test compound **61** was administered to Group III, and group IV at 10, and 20 mg/kg doses respectively. Group V served as carrageenan group for anti-inflammatory study. Both test and reference compounds were suspended in 0.1% w/v CMC-Na (carboxymethyl cellulose sodium) in normal saline and administered to fasting rats by daily oral dose for 7 successive days. On the 7th day anti-inflammatory activity of the compound **61** was assessed by classical carrageenan-induced paw edema model [5,39]. 1 h after administration of the doses, subplantar injection of freshly prepared 1% w/v carrageenan solution (150 μl) in normal saline induced acute inflammation in the hind paw. The paw volume was measured using vernier caliper prior to carrageenan injection and then

at 1, 2, 4, and 6 h after injection. The anti-inflammatory effect was determined as the difference in the reduction of paw volume between the groups received carrageenan alone and carrageenan with treatment. After 6 h, the animals were sacrificed by cervical dislocation. Hind paws were collected below the ankle and stored at –80 °C until assayed. The stomach was removed and an incision was made longitudinally along the greater curvature and cleaned with cooled saline. The gastric mucosa was inspected for any evidence of ulcer under the magnifying lens. Besides, histological studies were performed using hematoxylin and eosin [40–42].

4.2.7. Determination of PGE₂ and LTB₄ levels in inflamed paws

Hind paws stored at –80 °C were brought to RT and tissues were separated by degloving the bone. Then the tissues were homogenized in ice-cold saline (5 ml) and suspended in acetone for 10 min at RT. After incubation, tissue homogenates were subsequently centrifuged at 2000g at 4 °C for 10 min. The aliquots of supernatant were subjected for the determination of PGE₂ and LTB₄ levels by ELISA technique using prostaglandin E₂ and leukotriene B₄ parameter Kits according to manufacturer's instruction [36,43]. (Catalog No. KGE004B & KGE006B, R&D systems, Inc. USA).

4.2.8. Total RNA isolation and cDNA conversion

Paw tissues for qRT-PCR were stabilized by RNA later technology (Qiagen, USA). Total RNA was extracted from control, test and standard paw tissues using Trizol Reagent (Invitrogen, USA) according to manufacturer's guidelines. RNA was quantified by measuring its absorption at A260/A280 nm by Nanodrop BioSpectrometer (Eppendorf BioSpectrometer®, USA). 2 μg of total RNA from all the samples were reverse transcribed using the Omniscript Reverse Transcription kit (Qiagen, USA) according to manufacturer's guidelines. In brief, the total reaction volume was 20 μl containing 2 μg total RNA, 10x buffer RT, 5 mM dNTP mix, 10 μM oligo dT primer (Qiagen), RNase inhibitor, Omniscript reverse transcriptase and RNase free water. The reaction was conducted at 37 °C for 60 min.

4.2.9. Gene expression analysis in Wistar rat

Expression of three target gene and one internal control (GAPDH) were measured by qPCR. Primer set for each gene (Table 5) was designed using NCBI primer BLAST software. All primers were procured from Eurofins Genomics India Pvt. Ltd. (Bangalore, India). cDNA reversely transcribed from rats treated with control, test and standard were used as the template for analyzing the expression of COX-1, COX-2 and 5-LOX genes and GAPDH. The amplifications were carried out in 0.2 ml qPCR 8-strips tubes with optical caps (Gunster Biotech Co., Ltd, Taiwan) using CFX96 Real-Time System (BIO-RAD, USA). The real-time PCR reactions were carried out in 25 μl reaction systems with TB Green Premix Ex Taq II, 12.5 μl (Takara Bio Inc., Japan), 200 ng forward primer (10 μM), 200 ng reverse primer (10 μM), and 2 μl cDNA template. Each reaction was performed in triplicate. Thermal cycling conditions were; initial denaturation 95 °C for 30 s, subsequently 40 cycles of denaturation at 95 °C for 10 s, annealing at 60 °C for 1 min, and a final extension at 95 °C for 10 s. A PCR product melt curve analysis was

Table 5
Primers used for the qRT-PCR study.

Sl No	Primer code	Primer Sequence (5'-3')	Product (bp)	Accession number
1	COX-1-F	GTACCAGGTGCTGGATGGAGA	72	NM_017043.4
	COX-1-R	GGTGGGTAGCGCATCAACAC		
2	COX-2 -F	CCCACTTCAAGGGAGTCTGG	87	NM_017232.3
	COX-2 -R	GTGATCTGGACGTCAACACG		
3	5-LOX-F	CCTGAGGGATGGATGTGCAA	79	XM_006237140.2
	5-LOX -R	TTCCAGTTCTTTCGCCTGT		
4	GAPDH-F	GGCCACGCTAATCTGACTTTC	85	XM_017592435.1
	GAPDH-R	ATACGGCCAAATCCGTTTCAC		

done by heating from 65 to 95 °C with increments of 0.5 s. Data analysis was performed with the BIORAD CFX Maestro™ 4.1.2 (Bio-Rad). The quantification of COX-1, COX-2, and 5-LOX gene expression was performed using the housekeeping gene GAPDH. The $2^{-\Delta\Delta Ct}$ method (Livak and Schmittgen, 2001) was used for gene expression ratio calculation [44–46]. Relative amounts of all target genes were expressed by normalizing to GAPDH and control genes levels.

4.2.10. Determination of antioxidant activity

4.2.10.1. DPPH free radical scavenging assay. The free radical scavenging properties of all the test compounds have been studied as described [20,35]. Briefly, equal volumes of freshly prepared DPPH (0.1 mM) and test compounds (20 μM) in methanol were mixed well and allowed to stand in dark at RT for 30 min. The absorbance was measured on UV-Visible spectrophotometer (Shimadzu, Japan) at 517 nm. Ascorbic acid served as the reference standard and triplicate experiments were carried out. The percent DPPH radical scavenging was calculated by the formula:

$$\% \text{ inhibition} = \frac{(A_0 - A_s)}{A_0} \times 100 \quad (1)$$

where A_0 = absorbance of the control and A_s = absorbance of the test or standard sample

4.2.10.2. H_2O_2 radical scavenging assay. The capability of the test compounds to scavenge H_2O_2 radical was calculated according to previously reported method with slight modification [35]. Briefly, 40 mM H_2O_2 solution was prepared in PBS of pH 7.4. 20 μM of test compounds dissolved in 1 ml DMSO was added to 1 ml of H_2O_2 and incubated at RT for 10 min. The concentration of H_2O_2 was determined spectrophotometrically at 230 nm against blank solution of PBS without H_2O_2 . Triplicate experiments were conducted and results are displayed as mean ± SD. The percentage of H_2O_2 scavenged by the test compounds and standard was determined by the formula (1).

4.2.10.3. Iron chelating assay. Iron (II) chelating ability of the synthesized compounds was assessed according to Chew et al. [47]. Briefly, 1 ml 0.1 mM ferrous sulphate, was added to 1 ml of test compound (20 μM), followed by 1 ml 0.25 mM ferrozine. The thoroughly mixed reaction mixture was allowed to stand for 10 min and absorbance was observed at 562 nm. All the readings were taken in triplicate and reported as mean ± SD. The iron (II) chelating property of the compounds was calculated by the formula (1). Where, control consists of 1 ml each of 75% methanol, ferrozine and ferrous sulphate.

4.2.10.4. Nitric oxide (NO) scavenging assay. Nitric oxide scavenging activity was assessed by previous reports [48]. Briefly, 0.8 ml of test compounds (20 μM) in methanol was mixed with 0.2 ml of sodium nitroprusside (5 mM in PBS, pH 7.4) and incubated at RT for 180 min under the light source. After incubation, 0.6 ml of the above mixture was added to 0.6 ml of Griess reagent. After 10 min incubation in dark, absorbance was measured at 546 nm. The nitrite radical generated in the presence or absence of test compounds was estimated by plotting a standard curve with known concentrations of sodium nitrite solution. Experiments were performed in triplicate and percentage of nitrite scavenging was calculated.

4.3. Molecular docking studies

To understand the mode of interaction of lead molecule at COX-2 and 5-LOX enzyme active sites, molecular docking simulation was carried out using AutoDockTools 1.5.6. Briefly, the compound **61** and reference drugs were generated using the Argus Lab 4.0.1 and energy was minimized using Swiss-Pdb viewer 4.1.0 software. The crystal structures of COX-2 (PDB ID: 5IKT) and 5-LOX enzymes (PDB ID: 3O8Y) were obtained from the protein data bank. The compounds were docked

to predefined active sites [20], where polar hydrogens and partial charges were added to protein and ligand by AutoDockTools. The Autogrid program executes an efficient grid-based algorithm which provides an exhaustive search inside the dimensions of the binding site cavity. Grid maps of 60 Å × 60 Å × 60 Å points were centered on the protein active sites. Ligand conformational search was performed by Lamarckian Genetic Algorithm. The genetic algorithm (GA) population size was fixed to 150, the number of GA evaluation as 2500000, and GA docking runs were set to 100. Each ligand was docked separately with the enzymes in order to achieve best binding conformation. After docking, the binding energies of the ligands at different enzyme active sites were analyzed. The H-bonding interaction, hydrophobic interaction and van der Waal's interaction were studied and explored by measuring the distance between the protein and ligand.

4.4. Statistical analysis

In this study, the experimental results were presented as the mean ± SD of three parallel experiments or otherwise mentioned in the experimental procedure. Animal experiment data were expressed as mean standard error (± SEM). Statistical evaluation was carried out by one way analysis of variance (ANOVA). Statistical significance is expressed as *p < 0.05, **p < 0.01, and ***p < 0.001.

Declaration of Competing Interest

The authors declare that they have no conflict of interest in the publication.

Acknowledgments

The authors sincerely acknowledge the financial support of the VIT Seed Grant that facilitated us to carry out this work and to get it completed successfully in due course of time. The financial support to Jaismy Jacob P from the CSIR, Govt. of India, through Senior Research Fellowship is gratefully acknowledged.

Appendix A. Supplementary material

Supplementary data to this article can be found online at <https://doi.org/10.1016/j.bioorg.2020.103882>.

References

- [1] P. Singh, J. Kaur, G. Singh, R. Bhatti, Triblock conjugates: identification of a highly potent anti-inflammatory agent, *J. Med. Chem.* 58 (2015) 5989–6001.
- [2] P.F. Lamie, W.A. Ali, V. Bazgier, L. Rárová, Novel N-substituted indole Schiff bases as dual inhibitors of cyclooxygenase-2 and 5-lipoxygenase enzymes: synthesis, biological activities in vitro and docking study, *Eur. J. Med. Chem.* 123 (2016) 803–813.
- [3] P.J. Jacob, S. Manju, K. Ethiraj, G. Elias, Safer anti-inflammatory therapy through dual COX-2/5-LOX inhibitors: a structure-based approach, *Eur. J. Pharm. Sci.* (2018).
- [4] K. Liaras, M. Fesatidou, A. Geronikaki, Thiazoles and thiazolidinones as COX/LOX inhibitors, *Molecules* 23 (2018) 685.
- [5] M.H. Abdelrahman, B.G. Youssif, A.H. Abdelazeem, H.M. Ibrahim, A.M. Abd El Ghany, L. Treambu, S.N.A. Bukhari, Synthesis, biological evaluation, docking study and ulcerogenicity profiling of some novel quinoline-2-carboxamides as dual COXs/LOX inhibitors endowed with anti-inflammatory activity, *Eur. J. Med. Chem.* 127 (2017) 972–985.
- [6] S.X. Sun, K.Y. Lee, C.T. Bertram, J.L. Goldstein, Withdrawal of COX-2 selective inhibitors rofecoxib and valdecoxib: impact on NSAID and gastroprotective drug prescribing and utilization, *Curr. Med. Res. Opin.* 23 (2007) 1859–1866.
- [7] S. Sinha, S. Manju, M. Doble, Chalcone-Thiazole Hybrids: rational design, synthesis and lead identification against 5-Lipoxygenase, *ACS Med. Chem. Lett.* (2019).
- [8] S. Kulkarni, V. Pal Singh, Licofelone-a novel analgesic and anti-inflammatory agent, *Curr. Top. Med. Chem.* 7 (2007) 251–263.
- [9] P. Kay-Mugford, K. Grimm, A. Weingarten, P. Brianceau, P. Lockwood, J. Cao, Effect of preoperative administration of tepoxalin on hemostasis and hepatic and renal function in dogs, *Veter. Therapeut.: Res. Appl. Veter. Med.* 5 (2004) 120–127.
- [10] X. Ye, W. Zhou, Y. Li, Y. Sun, Y. Zhang, H. Ji, Y. Lai, Darbufelone, a novel anti-inflammatory drug, induces growth inhibition of lung cancer cells both in vitro and

- in vivo, *Cancer Chemother. Pharmacol.* 66 (2010) 277–285.
- [11] Y. Lai, L. Ma, W. Huang, X. Yu, Y. Zhang, H. Ji, J. Tian, Synthesis and biological evaluation of 3-[4-(amino/methylsulfonyl) phenyl] methylene-indolin-2-one derivatives as novel COX-1/2 and 5-LOX inhibitors, *Bioorg. Med. Chem. Lett.* 20 (2010) 7349–7353.
- [12] Y. Huang, B. Zhang, J. Li, H. Liu, Y. Zhang, Z. Yang, W. Liu, Design, synthesis, biological evaluation and docking study of novel indole-2-amide as anti-inflammatory agents with dual inhibition of COX and 5-LOX, *Eur. J. Med. Chem.* 180 (2019) 41–50.
- [13] Z. Li, Z.-C. Wang, X. Li, M. Abbas, S.-Y. Wu, S.-Z. Ren, Q.-X. Liu, Y. Liu, P.-W. Chen, Y.-T. Duan, Design, synthesis and evaluation of novel diaryl-1, 5-diazoles derivatives bearing morpholine as potent dual COX-2/5-LOX inhibitors and antitumor agents, *Eur. J. Med. Chem.* 169 (2019) 168–184.
- [14] R.N. Sharma, F.P. Xavier, K.K. Vasu, S.C. Chaturvedi, S.S. Pancholi, Synthesis of 4-benzyl-1, 3-thiazole derivatives as potential anti-inflammatory agents: an analogue-based drug design approach, *J. Enzyme Inhib. Med. Chem.* 24 (2009) 890–897.
- [15] R.K. Sathya, S. Jagadish, T. Swaroop, N. Ashwini, K. Harsha, K. Rangappa, Anti-oxidant and anti-inflammatory activities of synthetic 2, 4-bis (aryl/heteroaryl)-5-acylthiazole derivatives, *Asian J. Biochem. Pharmaceut. Res.* 4 (2014) 316–327.
- [16] M.T. Chhabria, S. Patel, P. Modi, P.S. Brahmshatriya, Thiazole: a review on chemistry, synthesis and therapeutic importance of its derivatives, *Curr. Top. Med. Chem.* 16 (2016) 2841–2862.
- [17] F.W. Bell, A.S. Cantrell, M. Hoegberg, S.R. Jaskunas, N.G. Johansson, C.L. Jordan, M.D. Kinnick, P. Lind, J.M. Morin Jr, Phenethylthiazolethiourea (PETT), compounds, a new class of HIV-1 reverse transcriptase inhibitors. 1. Synthesis and basic structure-activity relationship studies of PETT analogs, *J. Med. Chem.* 38 (1995) 4929–4936.
- [18] E.S. Taher, T.S. Ibrahim, M. Fares, A.M. AL-Mahmoudy, A.F. Radwan, K.Y. Orabi, O.I. El-Sabbagh, Novel benzenesulfonamide and 1, 2-benzisothiazol-3 (2H)-one-1, 1-dioxide derivatives as potential selective COX-2 inhibitors, *Eur. J. Med. Chem.* 171 (2019) 372–382.
- [19] I. Apostolidis, K. Liaras, A. Geronikaki, D. Hadjipavlou-Litina, A. Gavalas, M. Soković, J. Glamčič, A. Čirić, Synthesis and biological evaluation of some 5-arylidene-2-(1, 3-thiazol-2-ylimino)-1, 3-thiazolidin-4-ones as dual anti-inflammatory/antimicrobial agents, *Bioorg. Med. Chem.* 21 (2013) 532–539.
- [20] S. Sinha, M. Doble, S. Manju, Design, synthesis and identification of novel substituted 2-amino thiazole analogues as potential anti-inflammatory agents targeting 5-lipoxygenase, *Eur. J. Med. Chem.* 158 (2018) 34–50.
- [21] S. Sinha, T. Sravanthi, S. Yuvaraj, S. Manju, M. Doble, 2-Amino-4-aryl thiazole: a promising scaffold identified as a potent 5-LOX inhibitor, *RSC Adv.* 6 (2016) 19271–19279.
- [22] M.M. El-Miligy, A.A. Hazzaa, H. El-Messmary, R.A. Nassra, S.A. El-Hawash, New hybrid molecules combining benzothiophene or benzofuran with rhodanine as dual COX-1/2 and 5-LOX inhibitors: Synthesis, biological evaluation and docking study, *Bioorg. Chem.* 72 (2017) 102–115.
- [23] R.A. Funnell, G.D. Meakins, J.M. Peach, S.J. Price, A study of three reactions leading to isomeric 2-(N, N-disubstituted amino) thiazol-5-yl ketones, *J. Chem. Soc., Perkin Trans. 1* (1987) 2311–2315.
- [24] J.C. Brindley, J.M. Caldwell, G.D. Meakins, S.J. Plackett, S.J. Price, N'-substituted N-acyl- and N-imidoyl-thioureas: preparation and conversion of N', N'-disubstituted compounds into 2-(N, N-disubstituted amino) thiazol-5-yl ketones, *J. Chem. Soc., Perkin Trans. 1* (1987) 1153–1158.
- [25] A.M. Plutín, A. Alvarez, R. Mocoelo, R. Ramos, E.E. Castellano, M.M. da Silva, W. Villarreal, F.R. Pavan, C.S. Meira, J.S. Rodrigues, Filho, Palladium (II)/N, N-disubstituted-N'-acylthioureas complexes as anti-Mycobacterium tuberculosis and anti-Trypanosoma cruzi agents, *Polyhedron* 132 (2017) 70–77.
- [26] A.M. Plutín, A. Alvarez, R. Mocoelo, R. Ramos, E.E. Castellano, M.M. Da Silva, L. Colina-Vegas, F.R. Pavan, A.A. Batista, Anti-Mycobacterium tuberculosis activity of platinum (II)/N, N-disubstituted-N'-acyl thiourea complexes, *Inorg. Chem. Commun.* 63 (2016) 74–80.
- [27] S. Saeed, N. Rashid, M. Ali, R. Hussain, P.G. Jones, Synthesis, spectroscopic characterization, crystal structure and pharmacological properties of some novel thiophene-thiourea core derivatives, *Eur. J. Chem.* 1 (2010) 221–227.
- [28] K. Jeyalakshmi, J. Haribabu, C. Balachandran, N.S. Bhuvanesh, N. Emi, R. Karvembu, Synthesis of Ru (ii)-benzene complexes containing aroylthiourea ligands, and their binding with biomolecules and in vitro cytotoxicity through apoptosis, *New J. Chem.* 41 (2017) 2672–2686.
- [29] K. Jeyalakshmi, J. Haribabu, N.S. Bhuvanesh, R. Karvembu, Half-sandwich RuCl₂ (η⁶-p-cymene) core complexes containing sulfur donor aroylthiourea ligands: DNA and protein binding, DNA cleavage and cytotoxic studies, *Dalton Trans.* 45 (2016) 12518–12531.
- [30] S. Rajappa, M.D. Nair, B.G. Advani, R. Sreenivasan, J.A. Desai, A general synthesis of thiazoles. Part 3. Comparative evaluation of different functionalised thioureas as precursors, *J. Chem. Soc., Perkin Trans. 1* (1979) 1762–1764.
- [31] B. Halliwell, J.M. Gutteridge, *Free Radicals in Biology and Medicine*, Oxford University Press, USA, 2015.
- [32] C. Kemal, P. Louis-Flamberg, R. Krupinski-Olsen, A.L. Shorter, Reductive inactivation of soybean lipoxygenase 1 by catechols: a possible mechanism for regulation of lipoxygenase activity, *Biochemistry* 26 (1987) 7064–7072.
- [33] P. Sivakumar, P. Prabhakar, M. Doble, Synthesis, antioxidant evaluation, and quantitative structure–activity relationship studies of chalcones, *Med. Chem. Res.* 20 (2011) 482–492.
- [34] M.A. Ebrahimzadeh, S.M. Nabavi, S.F. Nabavi, F. Bahramian, A.R. Bekhradnia, Antioxidant and free radical scavenging activity of *H. officinalis* L. var. *angustifolius*, *V. odorata*, *B. hircana* and *C. speciosum*, *Pak. J. Pharm. Sci.* 23 (2010) 29–34.
- [35] J.P. Adjimini, P. Asare, Antioxidant and free radical scavenging activity of iron chelators, *Toxicol. Rep.* 2 (2015) 721–728.
- [36] G.-L. Xu, F. Liu, G.-Z. Ao, S.-Y. He, M. Ju, Y. Zhao, T. Xue, Anti-inflammatory effects and gastrointestinal safety of NNU-hdpa, a novel dual COX/5-LOX inhibitor, *Eur. J. Pharmacol.* 611 (2009) 100–106.
- [37] P. Singh, P. Prasher, P. Dhillon, R. Bhatti, Indole based peptidomimetics as anti-inflammatory and anti-hyperalgesic agents: dual inhibition of 5-LOX and COX-2 enzymes, *Eur. J. Med. Chem.* 97 (2015) 104–123.
- [38] A. Ganguly, O. Bhatnagar, Effect of bilateral adrenalectomy on production of restraint ulcers in the stomach of albino rats, *Can. J. Physiol. Pharmacol.* 51 (1973) 748–750.
- [39] L. George, T. Ramasamy, V. Manickam, S.K. Iyer, V. Radhakrishnan, Novel phenanthridine (PHE-4i) derivative inhibits carrageenan-induced rat hind paw oedema through suppression of hydrogen sulfide, *Inflammopharmacology* 24 (2016) 173–180.
- [40] S.K. Shrivastava, P. Srivastava, R. Bandresh, P.N. Tripathi, A. Tripathi, Design, synthesis, and biological evaluation of some novel indolizine derivatives as dual cyclooxygenase and lipoxygenase inhibitor for anti-inflammatory activity, *Bioorg. Med. Chem.* 25 (2017) 4424–4432.
- [41] A. Ganguly, A method for quantitative assessment of experimentally produced ulcers in the stomach of albino rats, *Experientia* 25 (1969) 1224–1224.
- [42] S. Sabiu, T. Garuba, T. Sunmonu, E. Ajani, A. Sulyman, I. Nurain, A. Balogun, Indomethacin-induced gastric ulceration in rats: protective roles of *Spondias mombin* and *Ficus exasperata*, *Toxicol. Rep.* 2 (2015) 261–267.
- [43] E.-S. Lee, B.C. Park, S.-H. Paek, Y.-S. Lee, A. Basnet, D.-Q. Jin, H.-G. Choi, C.S. Yong, J.-A. Kim, Potent analgesic and anti-inflammatory activities of 1-furan-2-yl-3-pyrrolidin-2-yl-propenone with gastric ulcer sparing effect, *Biol. Pharm. Bull.* 29 (2006) 361–364.
- [44] K.J. Livak, T.D. Schmittgen, Analysis of relative gene expression data using real-time quantitative PCR and the 2⁻ΔΔCT method, *Methods*, 25 (2001) 402–408.
- [45] K. Karthikeyan, R. Sudhakaran, Experimental horizontal transmission of *Enterocytozoon hepatopenaei* in post-larvae of whiteleg shrimp, *Litopenaeus vannamei*, *J. Fish Dis.* 42 (2019) 397–404.
- [46] P. Dhananjayulu, R.B. Boga, A. Mehta, Inhibition of aflatoxin B1 biosynthesis and down regulation of aflR and aflB genes in presence of benzimidazole derivatives without impairing the growth of *Aspergillus flavus*, *Toxicol* 170 (2019) 60–67.
- [47] Y.-L. Chew, J.-K. Goh, Y.-Y. Lim, Assessment of in vitro antioxidant capacity and polyphenolic composition of selected medicinal herbs from Leguminosae family in Peninsular Malaysia, *Food Chem.* 116 (2009) 13–18.
- [48] T. Chai, M. Mohan, H. Ong, F. Wong, Antioxidant, iron-chelating and anti-glucosidase activities of *Typha domingensis* Pers (Typhaceae), *Trop. J. Pharm. Res.* 13 (2014) 67–72.